



Mapping the Interface of a GPCR Dimer: A Structural Model of the A_{2A} Adenosine and D₂ Dopamine Receptor Heteromer

OPEN ACCESS

Edited by:

Dominique Massotte,

UPR3212 Institut des Neurosciences
Cellulaires et Intégratives (INCI),
France

Reviewed by:

Peter Vanhoutte,

Centre National de la Recherche
Scientifique (CNRS), France

Ahmed Hasbi,

University of Toronto, Canada

Juan Fernandez-Recio,

Barcelona Supercomputing Center,
Spain

Francesca Fanelli,

Università degli Studi di Modena e
Reggio Emilia, Italy

*Correspondence:

Kjell Fuxe

kjell.fuxe@ki.se

Jens Carlsson

jens.carlsson@icm.uu.se

†These authors have contributed
equally to this work

Specialty section:

This article was submitted to
Neuropharmacology,
a section of the journal
Frontiers in Pharmacology

Received: 08 February 2018

Accepted: 10 July 2018

Published: 30 August 2018

Citation:

Boroto-Escuela DO, Rodriguez D,
Romero-Fernandez W, Kapla J,
Jaiteh M, Ranganathan A, Lazarova T,
Fuxe K and Carlsson J (2018)
Mapping the Interface of a GPCR
Dimer: A Structural Model of the A_{2A}
Adenosine and D₂ Dopamine
Receptor Heteromer.
Front. Pharmacol. 9:829.
doi: 10.3389/fphar.2018.00829

Dasiel O. Boroto-Escuela^{1†}, *David Rodriguez*^{2†}, *Wilber Romero-Fernandez*³, *Jon Kapla*³, *Mariama Jaiteh*³, *Anirudh Ranganathan*², *Tzvetana Lazarova*⁴, *Kjell Fuxe*^{1*} and *Jens Carlsson*^{3*}

¹ Department of Neuroscience, Karolinska Institute, Stockholm, Sweden, ² Science for Life Laboratory, Department of Biochemistry and Biophysics, Stockholm University, Stockholm, Sweden, ³ Science for Life Laboratory, Department of Cell and Molecular Biology, Uppsala University, Uppsala, Sweden, ⁴ Department of Biochemistry and Molecular Biology, Institute of Neuroscience, Faculty of Medicine, Autonomous University of Barcelona, Barcelona, Spain

The A_{2A} adenosine (A_{2A}R) and D₂ dopamine (D₂R) receptors form oligomers in the cell membrane and allosteric interactions across the A_{2A}R–D₂R heteromer represent a target for development of drugs against central nervous system disorders. However, understanding of the molecular determinants of A_{2A}R–D₂R heteromerization and the allosteric antagonistic interactions between the receptor protomers is still limited. In this work, a structural model of the A_{2A}R–D₂R heterodimer was generated using a combined experimental and computational approach. Regions involved in the heteromer interface were modeled based on the effects of peptides derived from the transmembrane (TM) helices on A_{2A}R–D₂R receptor–receptor interactions in bioluminescence resonance energy transfer (BRET) and proximity ligation assays. Peptides corresponding to TM-IV and TM-V of the A_{2A}R blocked heterodimer interactions and disrupted the allosteric effect of A_{2A}R activation on D₂R agonist binding. Protein–protein docking was used to construct a model of the A_{2A}R–D₂R heterodimer with a TM-IV/V interface, which was refined using molecular dynamics simulations. Mutations in the predicted interface reduced A_{2A}R–D₂R interactions in BRET experiments and altered the allosteric modulation. The heterodimer model provided insights into the structural basis of allosteric modulation and the technique developed to characterize the A_{2A}R–D₂R interface can be extended to study the many other G protein-coupled receptors that engage in heteroreceptor complexes.

Keywords: G protein-coupled receptor, D₂ dopamine receptor, A_{2A} adenosine receptor, heteroreceptor complex, dimerization, dimer interface, allosteric modulation

INTRODUCTION

G protein-coupled receptors (GPCRs) play essential roles in physiological processes and are important therapeutic targets (Lefkowitz, 2004; Lagerstrom and Schioth, 2008). The vast majority of the research efforts that have been made to understand GPCR signaling was performed under the assumption that these membrane proteins function as monomers.

Contrary to this view, there is now evidence suggesting that many GPCRs form homo- and heteromers at the cell surface (Franco et al., 2000; Overton and Blumer, 2000; Angers et al., 2001; Han et al., 2009; Hasbi et al., 2009, 2017; Navarro et al., 2010; Vidi et al., 2010; Borroto-Escuela et al., 2014; Fuxe et al., 2014; Meng et al., 2014; Marsango et al., 2015; Martinez-Munoz et al., 2016; Rico et al., 2017). At the molecular level, GPCR signaling is hence not only determined by conformational changes induced by agonist binding, but is also allosterically modulated by interactions with other receptors. Further characterization of the influence of receptor–receptor interactions on signaling will be crucial for understanding GPCR function and could lead to development of novel drugs.

A prototypical GPCR heteromer is the one formed by the A_{2A} adenosine receptors (A_{2A}R) and D₂ dopamine receptors (D₂R) (Fuxe et al., 2010). *In vitro* experiments demonstrated that activation of the A_{2A}R reduces D₂R high affinity binding of agonists, suggesting that allosteric receptor–receptor interactions in the plasma membrane influence D₂R signaling (Ferre et al., 1991). This was further supported by the demonstration that the A_{2A}R and D₂R form heteroreceptor complexes with antagonistic receptor–receptor interactions in living cells and in brain tissue (Hillion et al., 2002; Fuxe et al., 2005). A considerable amount of experimental data, including biophysical, biochemical, chemical neuroanatomical, and behavioral studies support the view that A_{2A}R–D₂R heteromerization plays an important functional role in the basal ganglia (Ferre et al., 1991; Yang et al., 1995; Dasgupta et al., 1996; Fenu et al., 1997; Hillion et al., 2002; Canals et al., 2003; Kamiya et al., 2003; Ciruela et al., 2004; Fuxe et al., 2005, 2007b, 2010; Azdad et al., 2009; Borroto-Escuela et al., 2010a,b, 2018; Navarro et al., 2010; Fernandez-Duenas et al., 2012; Cordomi et al., 2015; Feltmann et al., 2018). The negative allosteric modulation exerted by A_{2A}R activation on D₂R signaling provided one mechanism contributing to the motor activation observed with general adenosine receptor antagonists (e.g., caffeine) and the neuroleptic effects of A_{2A}R agonists (Fuxe et al., 2007a). For this reason, the A_{2A}R–D₂R heteroreceptor complex represents a new therapeutic target for disorders treated with drugs interacting with the D₂R, such as neurodegenerative diseases, schizophrenia, and drug addiction (Borroto-Escuela et al., 2016b). For example, A_{2A}R antagonists should *inter alia* enhance dopaminergic signaling by blocking A_{2A}R activation by endogenous adenosine in A_{2A}R–D₂R oligomers, thereby reducing the negative allosteric modulation of the D₂R protomer (Fuxe et al., 2015). This may contribute to the antiparkinsonian effects observed after treatment with A_{2A}R antagonists, such as reduction of bradykinesia, motor fluctuations, and dyskinesia associated with chronic L-DOPA treatment (Schwarzschild et al., 2006; Armentero et al., 2011).

Despite the thorough characterization of GPCR heteromers by biophysical and biochemical methods (Angers et al., 2001; Vidi et al., 2010; Fernandez-Duenas et al., 2012; Borroto-Escuela et al., 2013; Fuxe et al., 2014; Marsango et al., 2015; Fuxe and Borroto-Escuela, 2016), the understanding of the structural basis of GPCR heteromerization and the associated negative and positive

cooperativity remains limited. A major advancement in this area was the recent determination of GPCR crystal structures, which enable generation of atomic resolution models for homo- and heteroreceptor complexes. Crystal structures for representative members from the adenosine (Liu et al., 2012) and dopamine (Chien et al., 2010; Wang et al., 2018) receptor families have recently been solved. In addition, a number of class A GPCRs have crystallized as homodimers (Murakami and Kouyama, 2008; Wu et al., 2010; Granier et al., 2012; Manglik et al., 2012; Huang et al., 2013), providing different plausible orientations of two monomers relative to each other. The rapidly increasing amount of structural data can now contribute to generation of models of GPCR dimers, which could improve understanding of allosteric modulation.

In this work, a combined computational and experimental approach to construct atomic resolution models of GPCR dimers was developed. In order to predict the structure of the A_{2A}R–D₂R heterodimer, regions involved in the interface were identified based on experiments utilizing peptides corresponding to the transmembrane (TM) helices of the A_{2A}R and D₂R. The effects of synthetic peptides corresponding to the seven TM helices of the A_{2A}R on A_{2A}R–D₂R heteromerization were assessed using bioluminescence resonance energy transfer (BRET) (Borroto-Escuela et al., 2013) and proximity ligation assays (PLAs). Combined with the corresponding BRET data for the seven TM peptides derived from the D₂R sequence (Borroto-Escuela et al., 2010b), an initial model of the A_{2A}R–D₂R heteromer was constructed computationally using protein–protein docking. The predicted heterodimer structure was refined using molecular dynamics (MD) simulations. The resulting A_{2A}R–D₂R structure was subsequently used to predict mutations in the dimer interface, which were evaluated experimentally to assess the model.

MATERIALS AND METHODS

Plasmid Constructs

The cDNA encoding the human D₂R, human A_{2A}R, and human A₁R cloned in pcDNA3.1+ were subcloned (without stop codons) in humanized pGFP²-N1 (PerkinElmer, Waltham, MA, United States), pEYFP-N1 (Clontech, Germany), and pRluc-N3 vectors (Packard Bioscience, Spain). The cDNA encoding human 3xHA-D₂R cloned in pcDNA3.1+ and human D₂R cloned in pGFP²-N1 (Perkin-Elmer, Spain) were used as template to generate the two mutants, Tyr192Ala^{5.41x42} and Leu207Ala^{5.56}/Lys211Ala^{5.60} [generic GPCR residue numbers indicated in superscript (Isberg et al., 2015)], by means of the QuickChangeTM site-directed mutagenesis kit (Stratagene, Netherlands) following the manufacturer's protocol. The other constructs used have been described previously (Borroto-Escuela et al., 2010a,b).

Cell Culture and Transfection

HEK293T cells (American Type Culture Collection, United States) were grown in Dulbecco's modified Eagle's medium supplemented with 2 mM L-glutamine, 100 units/ml

penicillin/streptomycin, and 10% (v/v) fetal bovine serum (FBS) at 37°C in an atmosphere of 5% CO₂. Cells were plated in 6-well plates at a concentration of 1×10^6 cells/well or in 75 cm² flasks and cultured overnight prior to transfection. Cells were transiently transfected using linear polyethylenimine (Polysciences Inc., United States). Rat primary striatal neuronal cells purchased from QBM Cell Science (Montreal, QC, Canada) were cultured in Neuro basal medium supplemented with 10% FBS, 2 mM GlutaMAX-1, 1 mM sodium pyruvate, 100 U/ml penicillin G, and 100 µg/ml streptomycin and B-27 supplement at 37°C in a humidified 10% CO₂ environment according to manufacturer's instructions.

TM Peptide Treatment

Synthetic peptides, representing each of the TM peptides of the human A_{2A}R, were obtained from Lazarova et al. (2004), Thevenin et al. (2005), Thevenin and Lazarova (2008), CASLO (Denmark) or Ana Spec Inc. (CA, United States) with ≥90% purity. The A_{2A}R TM-I peptide consisted of residues 8–32 (VYITVELAIAVLAILGNVLCWAVW); TM-II peptide of residues 43–66 (YFVVSLLAAADIAGVLAIPFAITI); TM-III peptide of residues 78–100 (LFIACFVLVLTQSSIFSLLAIAI); TM-IV peptide of residues 121–143 (AKGIIAICWVLSFAIGLTPMLGW); TM-V peptide of residues 174–198 (MNYMVYFNFFACVLVPLLLMLGVYL); TM-VI peptide of residues 235–261 (LAIIVGLFALAWLPLHIINCFTFFAPD); and TM-VII peptide of residues 267–291 (LWLMYLAIVLSHTNSVVPFIYAYR). A di-, tri- or quaternary basic sequence (KK, KKK, or RKKK) was introduced at the N- and C-terminal to ensure incorporation into the plasma membrane of cells, as demonstrated previously (Borroto-Escuela et al., 2012, 2018). The synthetic peptide representing TM-V of the 5-HT_{1A} receptor was described previously (Borroto-Escuela et al., 2012, 2015a,b). Immediately before use, the peptides were solubilized in dimethyl sulfoxide (DMSO) and diluted in the corresponding cell culture medium to yield a final concentration of 1% DMSO. We verified that, for each tested concentration of DMSO alone, no effect on cell viability was observed. Cells were incubated with the above mentioned peptides at 37°C for 2 h prior to performing BRET analysis, *in situ* PLA assays or binding assays.

BRET¹ Assays

In the BRET¹ assays, the receptors of interest were fused to either Renilla luciferase (RLuc) or yellow fluorescent protein (YFP). Detection of dimer interactions is based on that RLuc oxidation of the substrate coelenterazine *h* leads to light emission with a peak at 480 nm, which results in excitation of YFP (excitation and emission maxima of 475 and 530 nm, respectively) if the receptors are in close proximity (Pfleger and Eidne, 2006). In the BRET¹ saturation assays (Borroto-Escuela et al., 2013), HEK293T cells were transiently co-transfected with constant amounts (1 µg) of plasmids encoding for D₂R^{RLuc} and increasing amounts (0.5–8 µg) of plasmids encoding for A_{2A}R^{YFP}. Forty-eight hours after transfection the cells were rapidly washed twice in PBS, detached, and resuspended in

the same buffer. Cell suspensions (20 µg proteins) were distributed in duplicate into 96-well microplates; black plates with transparent bottom (Corning 3651, Corning, Stockholm, Sweden) for fluorescence measurement or white plates with white bottom (Corning 3600) for BRET determination. For BRET¹ ratio measurement, coelenterazine *h* substrate (Molecular Probes, Eugene, OR, United States) was added at a final concentration of 5 µM. Readings were performed after 1 min and the BRET signal was detected using the POLARstar Optima plate reader (BMG Lab Technologies, Offenburg, Germany) that allows the sequential integration of the signals detected with two filter settings. Transfected HEK293T cells were incubated with 0.1 µM of the A_{2A}R TM-V peptide at 37°C for 2 h prior to performing BRET¹ analysis. Data were then represented as a normalized netBRET¹ ratio versus the fluorescence value obtained from the YFP, normalized with the luminescence value of D₂R^{RLuc} expression 10 min after *h*-coelenterazine incubation. The normalized netBRET¹ ratio was defined as the BRET ratio for co-expressed RLuc and YFP constructs normalized against the BRET ratio for the RLuc expression construct alone in the same experiment: netBRET¹ ratio = [(YFP emission at 530 ± 10 nm)/(RLuc emission 485 ± 10 nm)] – cf. The correction factor, cf. corresponds to (emission at 530 ± 10 nm)/(emission at 485 ± 10 nm) found with the receptor-RLuc construct expressed alone in the same experiment. BRET isotherms were fitted using a non-linear regression equation assuming a single binding site, which provided BRET_{max} and netBRET_{max} values. The maximal value of BRET (BRET_{max} or netBRET_{max}) corresponds to the situation when all available donor molecules are paired up with acceptor molecules.

To assess specificity of the peptides, HEK293T cells were transiently co-transfected with plasmids encoding for D₂R^{RLuc} or A_{2A}R^{RLuc} and A_{2A}R^{YFP} (pcDNA ratio 1:1, 1 µg cDNA each). Forty-eight hours after transfection the cells were incubated with 10 µM of the A_{2A}R TM-IV peptide, or 0.1 µM of the A_{2A}R TM-V peptide, or 0.1 µM of the 5-HT_{1A} TM-V peptide at 37°C for 2 h prior to performing BRET¹ analysis. The netBRET signal was detected as described above.

In the BRET¹ competition assays, HEK293T cells transiently co-transfected with constant amounts (1 µg) of plasmids encoding for D₂R^{RLuc} and A_{2A}R^{YFP} were incubated with each of the seven A_{2A}R TM peptides at 37°C for 2 h prior to performing BRET¹ analysis. The netBRET signal was detected as described above.

BRET² Saturation Assays

In the BRET² assays, the receptors of interest were fused to either RLuc or green fluorescent protein 2 (GFP2). Detection of dimer interactions is based on that RLuc oxidation of coelenterazine 400a (DeepBlueC) leads to light emission with a peak at 395 nm, which results in excitation of GFP² (excitation and emission maxima of 400 and 510 nm, respectively) if the receptors are in close proximity (Pfleger and Eidne, 2006). The BRET² saturation assays (Borroto-Escuela et al., 2013) were carried out using plasmids encoding for A_{2A}R^{RLuc} and either

3xHA-D₂R^{GFP2}, 3xHA-D₂R^{GFP2}(Tyr192Ala^{5.41x42}) or 3xHA-D₂R^{GFP2}(Leu207Ala^{5.56}/Lys211Ala^{5.60}), respectively. Forty-eight hours after transfection, HEK293T cells transiently transfected with constant (1 μg) or increasing amounts (0.12–7 μg) of plasmids encoding for A_{2A}R^{Rluc} and either 3xHA-D₂R^{GFP2}, 3xHA-D₂R^{GFP2}(Tyr192Ala^{5.41x42}) or 3xHA-D₂R^{GFP2}(Leu207Ala^{5.56}/Lys211Ala^{5.60}), respectively, were rapidly washed twice in PBS, detached, and resuspended in the same buffer. Cell suspensions (20 μg protein) were distributed in duplicate into the 96-well microplates; black plates with a transparent bottom (Corning 3651) (Corning, Stockholm, Sweden) for fluorescence measurement or white plates with a white bottom (Corning 3600) for BRET determination. For BRET² measurement, DeepBlueC substrate (VWR, Sweden) was added at a final concentration of 5 μM, and readings were performed after 1 min using the POLARstar Optima plate-reader (BMG Lab Technologies, Offenburg, Germany) that allows the sequential integration of the signals detected with two filter settings. The netBRET² ratio was defined as the BRET ratio for co-expressed Rluc and GFP² constructs normalized against the BRET ratio for the Rluc expression construct alone: netBRET² ratio = [(YFP emission at 515 ± 30 nm)/(Rluc emission 410 ± 80 nm)] – cf. The correction factor, cf, corresponds to (emission at 515 ± 30 nm)/(emission at 410 ± 80 nm) found with the receptor-Rluc construct expressed alone in the same experiment. The maximal value of BRET (BRET²max or netBRET²max) corresponds to the situation when all available donor molecules are paired up with acceptor molecules (Fuxe et al., 2010). The specificities of A_{2A}R–D₂R interactions were assessed by comparison with co-expression of A₁R^{Rluc} and D₂R^{GFP2}.

***In situ* Proximity Ligation Assay**

HEK293T cells transiently co-transfected with constant amounts (1 μg) of plasmids encoding for A_{2A}R and D₂R and rat primary striatal neuronal cells were employed to study the effect of TM peptides on A_{2A}R–D₂R complexes by means of *in situ* PLA. Furthermore, to study the effect of D₂R mutants on A_{2A}R–D₂R complexes by means of *in situ* PLA, HEK293T cells were also transiently co-transfected with constant amounts (1 μg) of plasmids encoding for A_{2A}R and 3xHA-D₂R or 3xHA-D₂R(Tyr192Ala^{5.41x42}) or 3xHA-D₂R(Leu207Ala^{5.56}/Lys211Ala^{5.60}). *In situ* PLA was performed using rabbit polyclonal anti-A_{2A}R (Abcam: ab3461 or Millipore: AB1559) and mouse monoclonal anti-D₂R (Millipore MABN53, clone 3D9) primary antibodies (for quality control of the antibodies, see Feltmann et al., 2018) and the Duolink *in situ* PLA detection kit (Sigma-Aldrich, Sweden), following the protocol described previously (Borroto-Escuela et al., 2012, 2016a, 2018; Feltmann et al., 2018). Primary striatal neuronal cells or transiently co-transfected HEK293T cells were incubated with 10 μM of the A_{2A}R TM-IV peptide or 0.1 μM of the A_{2A}R TM-V peptide at 37°C for 2 h prior to performing cell fixation with 3.7% formaldehyde solution (Sigma-Aldrich, Stockholm, Sweden). PLA control experiments employed only one primary

antibody or cells transfected with cDNAs encoding only one type of receptor. The PLA signal was visualized and quantified by using a TCS-SL confocal microscope (Leica, United States) and the Duolink Image Tool software. High magnifications of the microphotograph were taken and visualized using multiple z-scan projection. It should be noted that if the confocal data acquisition is performed as a multiple z-scan some positive PLA blobs/clusters may appear to be inside the nuclear blue stained DAPI area despite being located on the cytoplasmic membrane.

Cell Surface Receptor Expression and Cellular Localization Analysis by Fluorescence Confocal Microscopy

HEK293T cells were transiently transfected with constant amounts (1 μg) of plasmids encoding for 3xHA-D₂R^{GFP2}, 3xHA-D₂R^{GFP2}(Tyr192Ala^{5.41x42}) or 3xHA-D₂R^{GFP2}(Leu207Ala^{5.56}/Lys211Ala^{5.60}). Then, cells were fixed in 4% paraformaldehyde for 10 min, washed with PBS containing 20 mM glycine, and mounted in a Vectashield immunofluorescence medium (Vector Laboratories, United Kingdom). Microscope observations were performed with a 40× oil immersion objective in a Leica TCS-SL confocal microscope (Leica, United States).

[³H]-Raclopride Competition Experiments

[³H]-Raclopride binding was displaced by quinpirole to determine the proportion of receptors in the high affinity state (RH), the high affinity (K_{i,High}), and low affinity (K_{i,Low}) values for the agonist binding sites from competition curves in HEK cells expressing either A_{2A}R/3xHA-D₂R, A_{2A}R/3xHA-D₂R(Tyr192Ala^{5.41x42}), or A_{2A}R/3xHA-D₂R(Leu207Ala^{5.56}/Lys211Ala^{5.60}). Membrane preparations (60 μg protein/ml) were incubated with increasing concentrations of quinpirole (0.001 nM to 1 μM) and 2 nM [³H]-raclopride (75 Ci/mmol, Novandi Chemistry AB, Sweden) in 250 μl of incubation buffer (50 mM Tris-HCl, 100 mM NaCl, 7 mM MgCl₂, 1 mM EDTA, 0.05% BSA, 1 mM DTT) and 0.3 IU/ml adenosine deaminase (EC 3.5.4.4, Sigma-Aldrich) for 90 min at 30°C in the presence or absence of 100 nM of the A_{2A}R agonist CGS-21680. Non-specific binding was defined by radioligand binding in the presence of 10 μM (+) butaclamol (Sigma-Aldrich, Sweden). The incubation was terminated by rapid filtration Whatman GF/B filters (Millipore Corp, Sweden) using a MultiScreenTM Vacuum Manifold 96-well followed by three washes (~250 μl per wash) with ice-cold washing buffer (50 mM Tris-HCl pH 7.4). The filters were dried, 5 ml of scintillation cocktail was added, and the amount of bound ligand was determined after 12 h by liquid scintillation spectrometry.

Statistical Analysis

The number of samples (*n*) in each experimental condition is indicated in figure legends. When two experimental conditions were compared, statistical analysis was performed using an unpaired *t*-test. Data from the competition experiments were analyzed by non-linear regression analysis. The changes induced

by CGS-21680 on RH, $K_{i,High}$, and $K_{i,Low}$ values were compared using one-way ANOVA. A p -value ≤ 0.05 was considered significant.

Homology Modeling

An atomic resolution structure of the D₂R was constructed using homology modeling based on a crystal structure of the D₃ subtype as template (PDB code 3PBL) (Chien et al., 2010). A set of 100 homology models was generated with MODELLER v9.10 (Sali and Blundell, 1993) based on a manually edited sequence alignment (**Supplementary Figure S1**) generated by the GPCR-ModSim webserver (Rodríguez et al., 2012). The D₂R residues Arg31^{1,29}-Tyr36^{1,34} were not present in the corresponding region of the template and alpha-helical restraints were added for these to extend TM-I. In addition, 140 residues from the intracellular loop 3 (IL3) of the D₂R were omitted by introducing a chain break between Arg222^{5,71} and Leu363^{6,25}. The ends of helices TM-V and TM-VI, which are connected by the IL3, were treated as independent. Selection of a final homology model was based on the DOPE scoring function (Shen and Sali, 2006), visual inspection, and the metrics available from the Molprobit server (Davis et al., 2007).

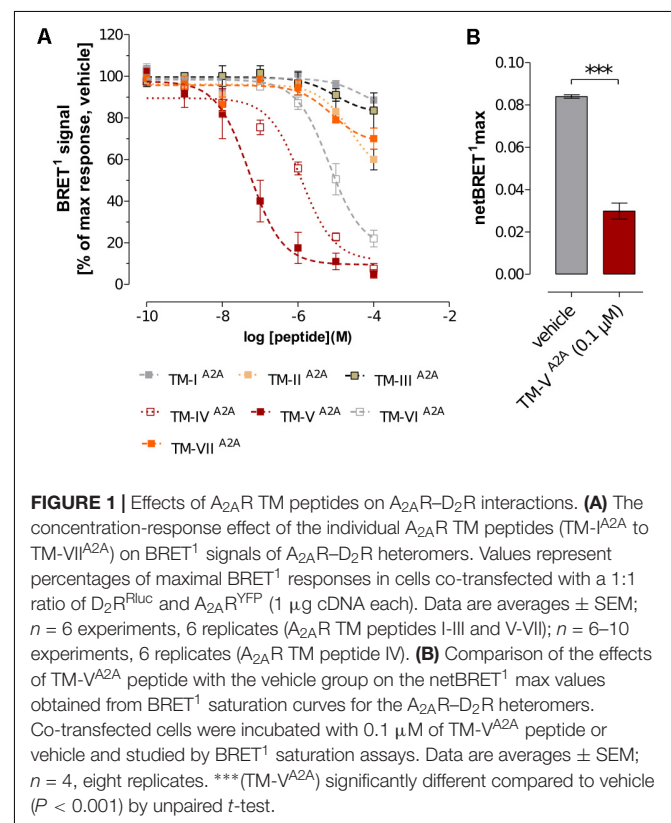
Protein–Protein Docking

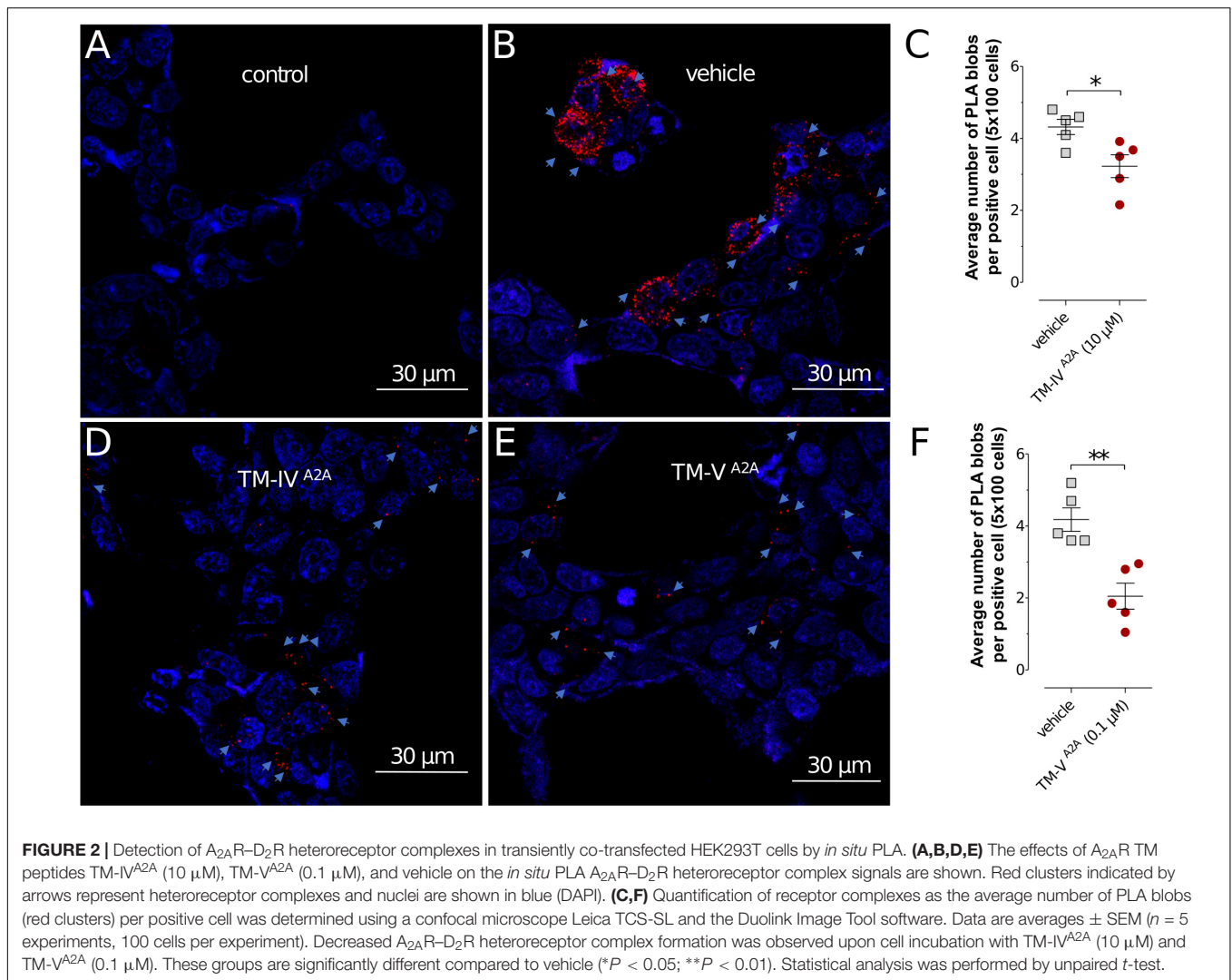
A crystal structure of the A_{2A}R (PDB code 4E1Y) (Liu et al., 2012) and the D₂R homology model were prepared for protein–protein docking with the program HADDOCK2.1 (Dominguez et al., 2003). The protonation states of ionizable residues (Asp, Glu, Arg, and Lys) were set to their most probable states at pH 7. Histidine protonation states were set by visual inspection on the basis of the hydrogen bonding network (**Supplementary Table S1**). Residues in the predicted dimer interface were used to guide protein–protein docking (**Supplementary Table S2**). A set of 1,000 configurations of the A_{2A}R–D₂R heterodimer was generated by rigid-body energy minimization. The 200 complexes with the best energy were refined and clustered by HADDOCK. Each A_{2A}R–D₂R complex was refined with MD sampling in the presence of explicit DMSO molecules to mimic the membrane environment. Subsequent to the determination of the first D₂R crystal structure (PDB code 6CM4) (Wang et al., 2018), the protein–protein docking was repeated with the same parameters. In this case, 10,000 configurations of the A_{2A}R–D₂R dimer were generated and 1,000 of these were refined. The resulting models were clustered (Rodríguez et al., 2012) based on superimposition to the A_{2A}R with a 7.5 Å RMSD cutoff and a minimum cluster size of four members.

MD Simulations

A model of the A_{2A}R–D₂R complex was prepared for all-atom MD simulations in GROMACS4.5.5 (Pronk et al., 2013). Prior to the MD simulations, the stretch of residues surrounding Ser197^{5,46x461} in the extracellular tip of TM-V of the D₂R was modified to preserve the alpha-helical secondary structure present in the D₃R template, which had slightly unfolded in the HADDOCK optimization of the heteromer complex. The dimer was inserted into a hydrated 1-palmitoyl-2-oleoylphosphatidylcholine (POPC) bilayer in gel

phase (equilibrated at 260 K). Water and lipid atoms overlapping with the protein were removed, and the simulation box walls were set to be 12 and 35 Å from the protein atoms in the Z and XY dimensions, respectively. A 0.15 M sodium concentration and neutralization of the system were accomplished by adding 100 sodium and 118 chloride ions to the system. The resulting hexagonal prism-shaped simulation box comprised 145,260 atoms, including 36,889 water and 438 lipid molecules, and had an initial volume of $156 \times 156 \times 99 \text{ \AA}^3$. MD simulations were performed using the half-ε double-pairlist method (Chakrabarti et al., 2010) to make the Berger parameters employed for the lipids (Berger et al., 1997) compatible with the OPLS-AA force field (Jorgensen et al., 1996) used for the protein atoms. As a part of the IL3 of the D₂R was excluded from modeling, C-terminal amide and N-terminal acetyl caps were added to avoid charge–charge interactions between the termini of residues Arg222 and Leu363, respectively. Similarly, the N-termini of both the A_{2A}R (Gly5^{1x31}) and D₂R (Tyr34^{1x32}) were capped. The system was solvated with SPC waters (Jorgensen et al., 1983). Bond lengths and angles for these molecules were constrained with the SETTLE algorithm (Miyamoto and Kollman, 1992), whereas the LINCS algorithm (Hess et al., 1997) was used to constrain bond lengths of proteins and lipids. Periodic-boundary conditions were applied in the NPT ensemble using the semiisotropic Parinello-Raman barostat (Parrinello and Rahman, 1981) (1 atm, coupling constant of 2 ps, isothermal compressibility constant of $4.5 \times 10^{-5} \text{ bar}^{-1}$) and the Nose–Hoover thermostat (310 K with three





independent coupling groups for proteins, lipids, and water plus ions). Lennard-Jones and coulombic interactions were explicitly considered within a 12 Å cutoff, whereas the particle mesh Ewald method was used for electrostatic interactions beyond that distance (Darden et al., 1993). The system was first minimized with the steepest descent algorithm and was then equilibrated using a time step of 2 fs by applying positional restraints only to protein atoms (**Supplementary Table S3**), which were gradually released during 10 ns. Three replicas with different initial random velocities were initiated from the last snapshot of the equilibration and 100 ns were then performed in each case.

RESULTS

Mapping of the TM Helices Involved in the A_{2A}R–D₂R Heterodimer Interface

Peptides corresponding to TM helices have been found to disrupt receptor–receptor interactions for GPCRs that form

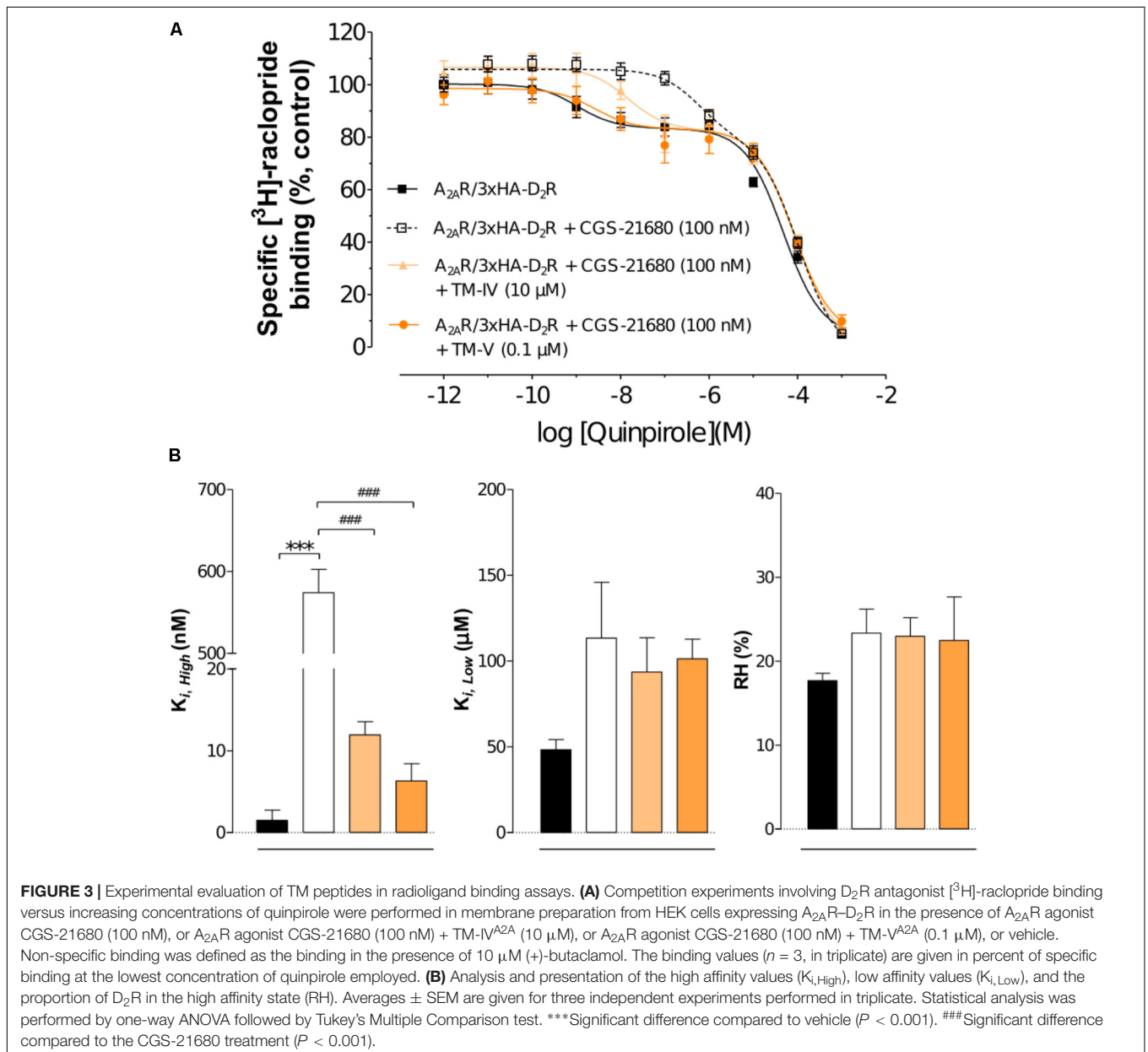
oligomers (Hebert et al., 1996; Ng et al., 1996; Borrito-Escuela et al., 2010b, 2012; Guitart et al., 2014; Lee et al., 2014; Jastrzebska et al., 2015; Vinals et al., 2015). The proposed mechanism of inhibition is that the helices are part of the protein–protein interface and are able to block oligomerization through competition with the other protomer. Structural information could thus be deduced by investigating the effects of the individual 14 TM helices of the two involved GPCRs on dimerization. In previous work, the ability of the TM helices of the D₂R to disrupt A_{2A}R–D₂R heteromerization was evaluated by means of quantitative BRET¹ assays (Borrito-Escuela et al., 2010b). The receptor–receptor interactions between the A_{2A}R labeled with YFP (A_{2A}R^{YFP}) and D₂R fused to RLuc (D₂R^{RLuc}) were characterized for the inhibition of the BRET¹ signal by the seven TM helices (TM-I^{D2} to TM-VII^{D2}) in concentration-response experiments. Addition of synthetic peptides TM-IV^{D2} and TM-V^{D2} resulted in a clear concentration-dependent reduction of the BRET¹ signal, leading to a nearly complete blockade at 1 to 10 μM. TM-VI^{D2} also

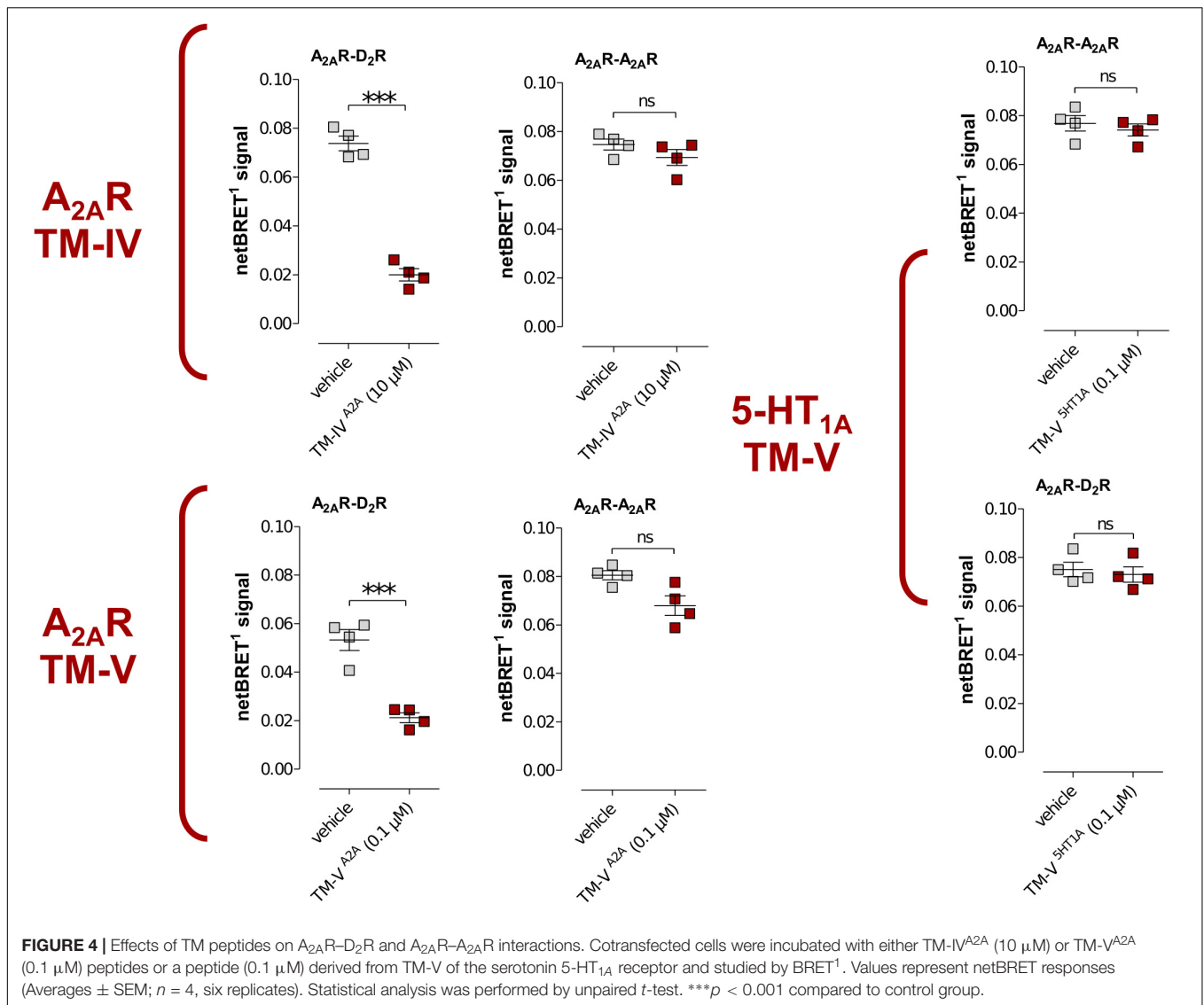
achieved some inhibition at these concentrations, but not to the same extent as TM-IV^{D2} and TM-V^{D2}. The remaining four peptides did not significantly influence A_{2A}R–D₂R heteromerization.

In the current work, the BRET¹ experiments were performed for the seven TM peptides of the A_{2A}R (TM-I^{A2A} to TM-VII^{A2A}), TM-IV^{A2A}, TM-V^{A2A}, and TM-VI^{A2A} displayed a concentration-dependent inhibition of the BRET¹ signal (Figure 1A). TM-V^{A2A} had the largest effect and A_{2A}R–D₂R dimerization was almost completely blocked at 1 μM. In a BRET saturation assay, TM-V^{A2A} clearly resulted in a significant reduction of the netBRET¹max values at 0.1 μM (Figure 1B). TM-IV^{A2A} and TM-VI^{A2A} also reduced the BRET¹ signal and reached close to full inhibition at 10 and 100 μM, respectively.

TM-IV^{A2A} and TM-V^{A2A} were also evaluated by *in situ* PLAs to characterize the disruption of A_{2A}R–D₂R heteroreceptor complexes in transiently co-transfected HEK293T cells (TM-IV^{A2A}, TM-V^{A2A}) and in rat striatal primary neuronal cell culture (TM-V^{A2A}). In line with the BRET¹ assays, the *in situ* PLA assay showed that the number of clusters of A_{2A}R–D₂R heteroreceptor complexes was reduced upon addition of 10 μM of TM-IV^{A2A} and 0.1 μM TM-V^{A2A} (Figure 2 and Supplementary Figure S2).

To evaluate the impact of the interfering peptides on the allosteric modulation within the A_{2A}R–D₂R heteromer, the affinity values for D₂R agonist quinpirole for D₂R were examined in [³H]-raclopride/quinpirole competition assays in HEK293T cells. The high affinity value ($K_{i,High}$), the low affinity value ($K_{i,Low}$), and the proportion of receptors in the high affinity





state (RH) were not significantly altered when cells expressing only the D₂R were treated with the TM-IV^{A2A} and TM-V^{A2A} peptides compared with the vehicle by one-way ANOVA (Supplementary Figure S3). The A_{2A}R agonist CGS-21680 decreased the affinity of the high affinity component of the D₂R agonist quinpirole in membrane preparations expressing A_{2A}R–D₂R, but the $K_{i,Low}$ and RH values were unaffected (Figure 3). Agonist binding to the high affinity state ($K_{i,High}$) was reduced from 1.05 ± 0.36 nM to 583 ± 27 nM by the A_{2A} agonist CGS-21680. Thus, the strong negative allosteric modulation exerted by the A_{2A}R agonist on the high affinity state of the wild type D₂R was validated. In contrast, the allosteric modulation was significantly reduced in the experiments carried out in the presence of the TM-IV^{A2A} and TM-V^{A2A} peptides. TM-V^{A2A} resulted in the strongest effect and there was a complete loss of allosteric modulation ($K_{i,High} = 2.65 \pm 0.52$ nM). TM-IV^{A2A} also counteracted the effect on the high affinity component, resulting in a $K_{i,High}$ of 14.69 ± 0.35 nM.

No differences in RH and $K_{i,Low}$ values were observed after the A_{2A}R agonist modulation or treatment of TM peptides (Figure 3).

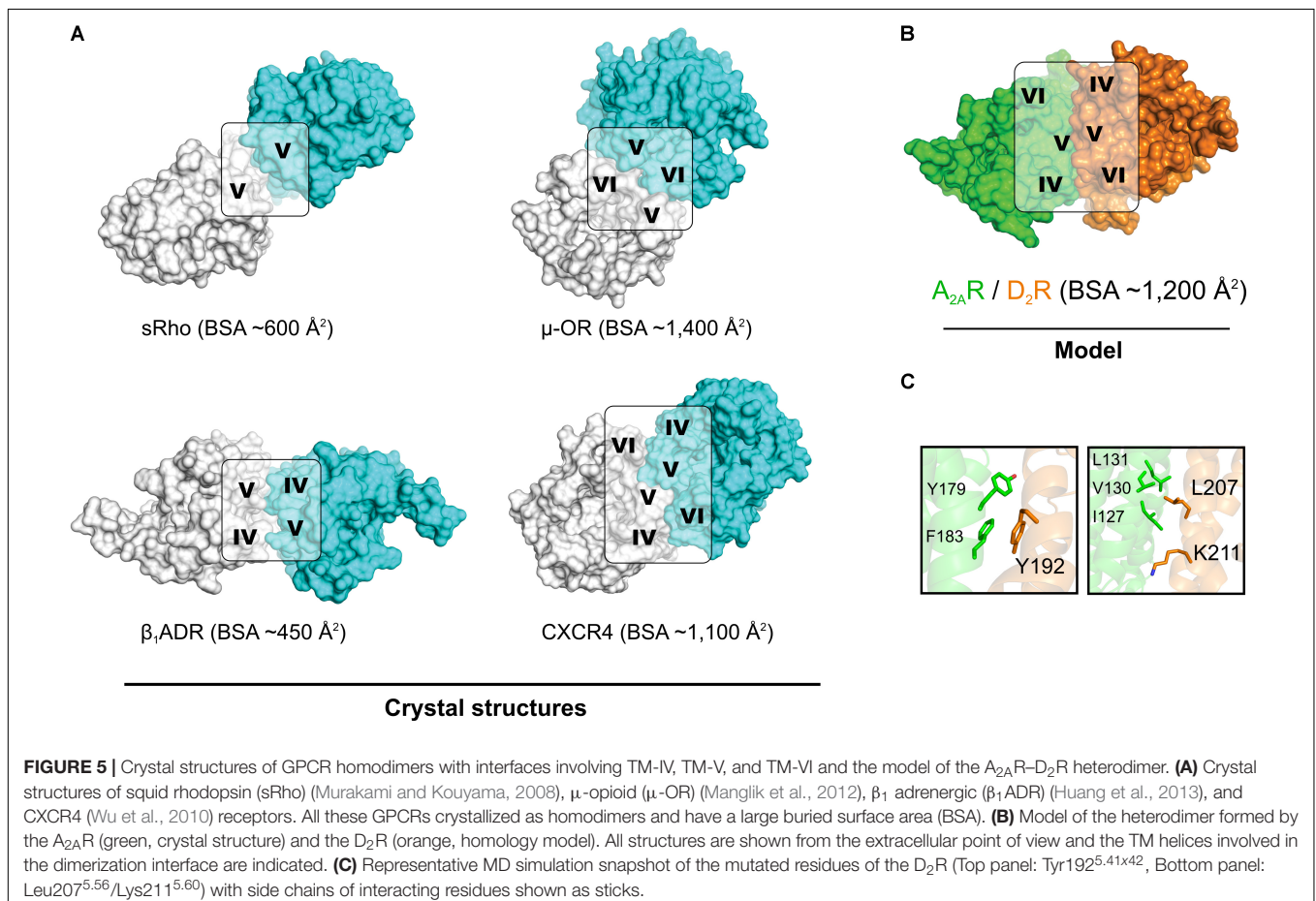
To investigate the specificity of the A_{2A}R TM peptides, BRET¹ experiments were also carried out for the A_{2A}R homodimer with a receptor population labeled with either YFP (A_{2A}R^{YFP}) or Rluc (A_{2A}R^{Rluc}), which were compared to the results obtained for the A_{2A}R–D₂R heterodimer. Each peptide was assayed at a single-point concentration of 10 μM (TM-IV^{A2A}) or 0.1 μM (TM-V^{A2A}) and, interestingly, the results were different for the homo- and heterodimer. As expected, TM-IV^{A2A} and TM-V^{A2A} significantly reduced the population of A_{2A}R–D₂R complexes. However, no significant reduction of the BRET¹ signal was observed for these two peptides in the case of A_{2A}R homodimer. Similarly, the use of a peptide corresponding to TM-V of the serotonin 5-HT_{1A} receptor (Borroto-Escuela et al., 2012) did not have any significant effect on the A_{2A}R–D₂R heteromer or A_{2A}R–A_{2A}R homomer interactions (Figure 4).

Experiment-Guided Modeling of the A_{2A}R–D₂R Heteroreceptor Complex

Modeling of the A_{2A}R–D₂R complex was guided by the BRET¹ data for the 14 TM peptides of the two protomers and dimer interactions observed in crystal structures of GPCRs. No crystal structures were available for heterodimers, but several class A GPCRs have been crystallized in homomeric arrangements, revealing different potential interfaces (**Figure 5A**) (Murakami and Kouyama, 2008; Wu et al., 2010; Granier et al., 2012; Manglik et al., 2012; Huang et al., 2013). The first cluster of observed dimer interfaces mainly involved TM-I, TM-II, and helix VIII and has, for example, been identified in crystal structures of the β₁ adrenergic (Huang et al., 2013), κ- and μ-opioid (Granier et al., 2012; Manglik et al., 2012) receptors. As no effects of TM-I or TM-II on A_{2A}R–D₂R heteromerization were observed in the BRET¹ assays, this interface was not further considered. A second set of interfaces involving TM-V and either TM-IV or TM-VI has been revealed by, e.g., crystal structures of squid rhodopsin (Murakami and Kouyama, 2008), CXCR4 (Wu et al., 2010), μ-opioid (Manglik et al., 2012), and β₁ adrenergic (Huang et al., 2013) receptors. The synthetic peptides corresponding to the same three helices of the D₂R and A_{2A}R disrupted A_{2A}R–D₂R heterodimerization in the BRET¹ assays (**Figure 1**) (Borroto-Escuela et al., 2010b). Visual inspection of the TM-IV/V/VI

interfaces observed in the crystal structures of the CXCR4, μ-opioid, and β₁ adrenergic receptors revealed that none of the observed dimers simultaneously involved all three helices to a significant extent. The μ-OR and squid rhodopsin receptor dimers had TM-V/VI and TM-V interfaces, respectively, but not TM-IV, which showed the largest effect among the synthetic peptides derived from the D₂R. The β₁ adrenergic receptor had a TM-IV/V interface, but the buried surface area (BSA) was relatively small (450 Å²). The CXCR4 receptor structure had strong interactions via TM-V and also involved TM-IV and TM-VI to a smaller extent, resulting in the largest BSA (~1,100 Å²).

In order to generate a model of the A_{2A}R–D₂R heterodimer, atomic resolution structures for the monomeric forms of each protomer were required. Multiple crystal structures of the A_{2A}R in monomeric form were available and the one with the highest resolution, which represented an inactive state conformation, was selected (Liu et al., 2012). At the initiation of this study, no crystal structure of the D₂R was available. Thus, a crystal structure of the D₃R (Chien et al., 2010) was used to generate a set of homology models of the D₂R in an inactive-like state. Due to the high sequence similarity to the D₃R, which shared 71% of the amino acids in the TM region with the D₂ subtype (**Supplementary Figure S1**), there was only a small variation among the models generated. The three best models, as judged



by DOPE score (Shen and Sali, 2006), were analyzed manually and one of these was selected as a starting point for modeling of the heterodimer. Models of the A_{2A}R–D₂R complex were first generated by structural superimposition of the monomers onto the available homodimer crystal structures with interfaces that involved TM-IV and TM-V. CXCR4 (Wu et al., 2010) was considered to be the best template for the A_{2A}R–D₂R heterodimer based on the large contact interface involving TM-V, but the resulting model only had weak interactions with TM-IV. Protein–protein docking with the program HADDOCK (Dominguez et al., 2003) was performed to identify interfaces that were in better agreement with the experimental data for the TM peptides. HADDOCK allows inclusion of experimental data to focus the docking calculation on a specific interface. Residues in TM-IV and TM-V were defined as being involved in the interface based on the BRET data and CXCR4-based model (Supplementary Table S2). The protein–protein docking was used to generate 200 models of the A_{2A}R–D₂R complex, which were clustered based on RMSD. The 10 most populated clusters are shown in Supplementary Figure S4 and were analyzed based on four criteria (Supplementary Table S4). The first two criteria required the receptors to be oriented in a parallel manner and correctly aligned with the plane of the membrane–solvent interface, which was fulfilled by 133 models from four different clusters. Among these, the heterodimer models in the sixth cluster were found to have the most extensive contacts involving TM-IV and TM-V and its centroid was selected for further consideration (Figure 5B and Supplementary Figure S5). The predicted A_{2A}R–D₂R interface had a total BSA of ~1,200 Å² and was overall similar, but not identical, to the model obtained by aligning to the CXCR4 homodimer crystal structure (Supplementary Figure S6). TM-V was the helix with the highest contribution to the dimer interface for both protomers. However, the selected structure had some rearrangements compared to CXCR4-based model that led to higher involvement of TM-IV.

MD Simulation Refinement of the A_{2A}R–D₂R Heterodimer Model

The A_{2A}R–D₂R heterodimer predicted by protein–protein docking was further explored using all-atom MD simulations in a hydrated lipid bilayer. The time-scales reachable by MD simulations are too short to observe major rearrangements of the dimer interface, structural changes related to activation of the receptors, or the influence of oligomerization on ligand binding. Therefore the goal of these calculations was to refine the predicted interface using a more realistic model of the biological environment. Three independent trajectories of the dimer model were generated, resulting in a total of 0.3 μs of unrestrained simulation. After a short equilibration (Supplementary Table S3), the overall root mean square deviation (RMSD) of the Cα atoms of the dimer increased slightly during the first ~40 ns of unrestrained simulation and then stabilized at an average of 3.3 Å, which is similar to the results obtained for a simulation study on the crystal structure of the CXCR4 homodimer (Rodriguez and Gutierrez-De-Teran, 2012). The largest structural changes were observed in TM-VII of the A_{2A}R and TM-I of the D₂R

whereas the dimer interface remained stable. The BSA changed only slightly during the simulation, with an average of 1,163 Å² for the last 50 ns of the three simulation replicas (Supplementary Figure S7 and Supplementary Table S5).

Snapshots from the MD simulations were analyzed to identify interactions between specific residues in the interface. To further evaluate the model, two D₂R mutants that probed interactions in either the N- or C-terminal ends of these helices were predicted (Figure 5C). The interaction interface at the top of TM-V was close to the orthosteric binding sites of both receptors. Tyr192^{5.41x42} of the D₂R was located just one helical turn from a set of residues (Ser193^{5.42x43}, Ser194^{5.43x44}, and Ser197^{5.46x46}) that has been proposed to play a role in the activation mechanism for monoamine-recognizing GPCRs (Warne et al., 2011). The side chain of Tyr192^{5.41x42} formed stacking interactions with a cluster of aromatic residues formed by Tyr179^{5.40x41} and Phe183^{5.44x45} in TM-V of the A_{2A}R, which were located only ~10 Å from the adenosine binding site. At the intracellular end of TM-V of the D₂R, interactions with residues in TM-IV and TM-V of the A_{2A}R were formed. Leu207^{5.56} of the D₂R interacted with Ile127^{4.48}, Val130^{5.51}, and Leu131^{4.52} of

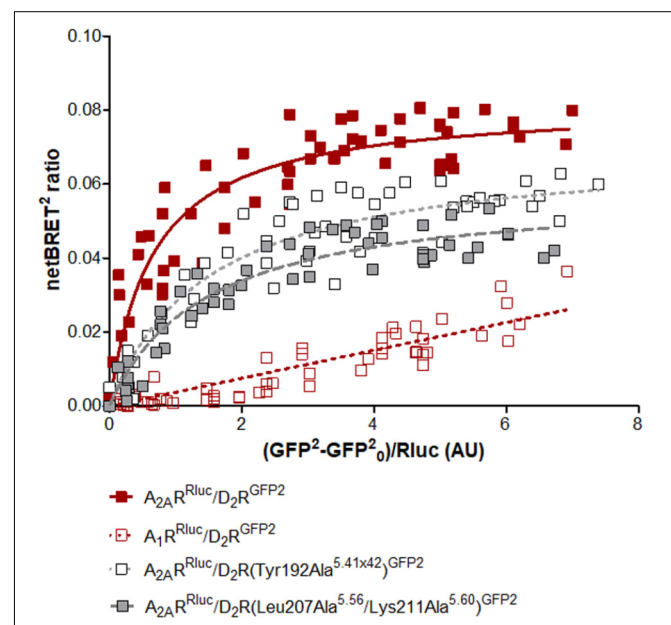
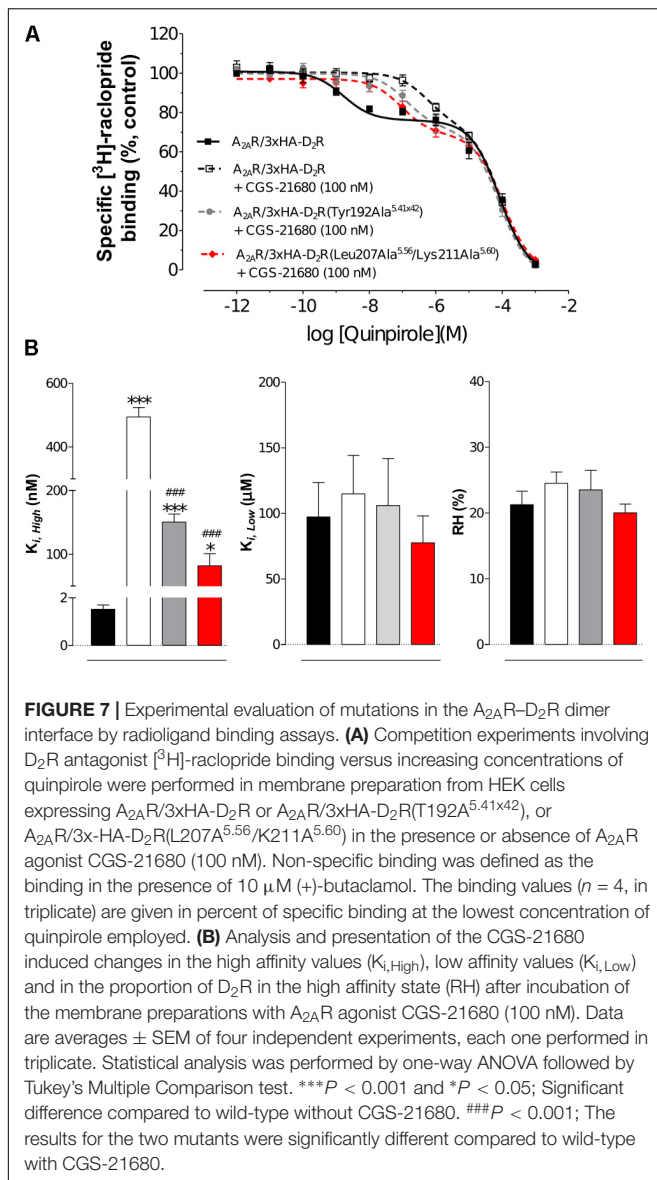


FIGURE 6 | Experimental evaluation of mutations in the A_{2A}R–D₂R dimer interface by BRET². BRET² saturation curves for the A_{2A}R–D₂R heterodimer for wild type and mutants of the D₂R. The normalized BRET² ratio, which was defined as the netBRET² ratio for co-expressed Rluc and GFP² constructs normalized against the netBRET² ratio for the Rluc expression construct alone in the same experiment, is plotted on the y-axis. The fluorescence value obtained from the GFP², normalized with the luminescence value of A_{2A}R^{Rluc} or A₁R^{Rluc} expression 10 min after *DeepBlueC* incubation, is plotted on the x-axis. GFP₀ is defined as the fluorescent emission values at 515 ± 30 nm of the cells which only expressed the Rluc construct. Data are averages ± SEM; n = 5, eight replicates. Statistical analysis was performed by unpaired *t*-test. The netBRET²max values of A_{2A}R–D₂R(Tyr192Ala^{5.41x42}) are significantly different compared to A_{2A}R–D₂R (*P* < 0.05) and the netBRET²max values of A_{2A}R–D₂R(Leu207Ala^{5.56}/Lys211Ala^{5.60}) are significantly different compared to A_{2A}R–D₂R (*P* < 0.01).



the A_{2A}R whereas the alkyl chain of Lys211^{5.60} formed van der Waals interactions with Ile127^{4.48} of the A_{2A}R. Based on these results, two mutants of the D₂R, Tyr192Ala^{5.41x42} and Leu207Ala^{5.56}/Lys211Ala^{5.60}, were predicted to reduce favorable dimer interactions and were selected for experimental evaluation.

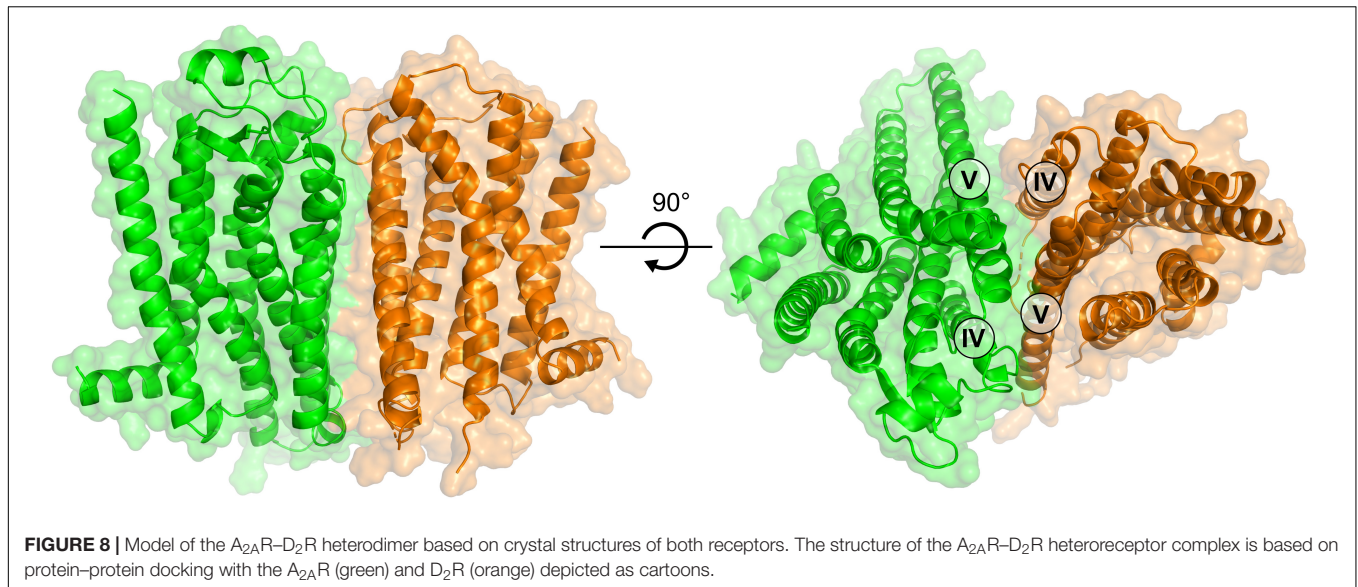
Experimental Evaluation of D₂R Mutations in the Predicted Heteromer Interface

To further probe the predicted role of TM-V of the D₂R in A_{2A}R–D₂R heteromerization, the Tyr192Ala^{5.41x42} and Leu207Ala^{5.56}/Lys211Ala^{5.60} D₂R mutants were evaluated experimentally in BRET², *in situ* PLA, and binding assays. No differences in cellular localization at the membrane level between the wild type and mutants of the D₂R were observed

(Supplementary Figure S8). The interactions between the wild type and mutant D₂R labeled with GFP2 with the A_{2A}R^{RLuc} were first assessed in BRET² saturation assays. Both the Tyr192Ala^{5.41x42} and Leu207Ala^{5.56}/Lys211Ala^{5.60} mutations reduced A_{2A}R–D₂R interactions and the largest effect was observed for the double mutant (*p* < 0.01, Figure 6). In contrast, no significant differences were observed between the wild type and mutant D₂R with the A_{2A}R protomer if the *in situ* PLA method was used (Supplementary Figure S9). In binding assays, the high affinity value (*K_{i,High}*) for D₂R agonist quinpirole for 3xHA-D₂R, 3xHA-D₂R(Tyr192Ala^{5.41x42}), and 3xHA-D₂R(Leu207Ala^{5.56}/Lys211Ala^{5.60}) were determined in [³H]-raclopride/quinpirole competition assays (1.65 ± 0.21 nM, 1.08 ± 0.34 nM, and 1.80 ± 0.22 nM, respectively). The high affinity value (*K_{i,High}*), the low affinity value (*K_{i,Low}*) and the proportion of receptors in the high affinity state (RH) were not significantly altered for the two D₂R mutants compared with the wild type D₂R by one-way ANOVA (Supplementary Figure S10). As expected, the A_{2A}R agonist CGS-21680 decreased the affinity of the high affinity component of the D₂R agonist quinpirole in membrane preparations expressing A_{2A}R/3xHA-D₂R whereas the *K_{i,Low}* and RH values were not significantly altered. The D₂R agonist binding to the high affinity state was reduced 300-fold by the A_{2A} receptor agonist CGS-21680 to 533 ± 23 nM. Significant A_{2A}R agonist induced reductions of the *K_{i,High}* value for quinpirole were also observed for the D₂R mutants, but not to the same degree as found in the wild type. The Tyr192Ala^{5.41x42} and Leu207Ala^{5.56}/Lys211Ala^{5.60} mutants had (*K_{i,High}*) values equal to 129 ± 21 nM and 90 ± 2 nM in the presence of A_{2A}R agonist, respectively. The ability of 3xHA-D₂R(Tyr192Ala^{5.41x42}) and 3xHA-D₂R(Leu207Ala^{5.56}/Lys211Ala^{5.60}) to respond to the negative allosteric modulation induced by the A_{2A}R agonist was hence significantly lower than for the wild type A_{2A}R/3xHA-D₂R complex. No significant differences in RH and *K_{i,Low}* values were observed (Figure 7).

Model of the A_{2A}R–D₂R Complex Based on Crystal Structures of Both Protomers

After the initial review of this paper, the first crystal structure of the D₂R was determined (Wang et al., 2018). This allowed us to assess the accuracy of the D₂R model and generate alternative interfaces of the A_{2A}R–D₂R dimer using protein–protein docking based on crystal structures of both receptors. Alignment of the D₂R homology model and crystal structure showed that the D₃R subtype was a good template for the prediction of the TM region (backbone RMSD = 1.2 Å). To assess the influence of using a D₂R homology model on our results and to further improve our model of the A_{2A}R–D₂R complex, the protein–protein docking calculations were carried out with the crystal structures. A total of 1,000 models were generated and the resulting clusters of potential interfaces were assessed using the same criteria as for the D₂R homology model (Supplementary Table S6). The third most populated cluster was compatible with membrane insertion and had a TM-IV/V interface. The interface RMSD between the cluster



center obtained from docking with the D₂R homology model (cluster 6, **Supplementary Table S4**) and crystal structure (cluster 3, **Supplementary Table S6**) was 4.6 Å. These models hence belonged to the same cluster of solutions (HADDOCK clustering cut-off < 7.5 Å) and the interfaces were very similar based on our criteria (**Supplementary Figure S11**). On the residue level, there were some differences in the interactions predicted by the two cluster centers, but the contacts made by the residues evaluated by mutagenesis (Tyr192Ala^{5,41x42} and Leu207Ala^{5,56}/Lys211Ala^{5,60}) were maintained in the A_{2A}R–D₂R complex obtained using the crystal structures (**Supplementary Figure S11**). A representative A_{2A}R–D₂R model obtained using crystal structures of both receptors is shown in **Figure 8**.

DISCUSSION

The main result of this study is that identification of dimer disrupting peptides derived from TM helices in combination with crystal structure data for GPCRs enabled the generation of atomic-resolution models of the A_{2A}R–D₂R heteroreceptor complex. A representative A_{2A}R–D₂R model was refined using MD simulations and mutations in the predicted interface reduced the propensity of the receptors to dimerize.

A key step toward understanding GPCR heteromerization is the identification of the regions involved in receptor–receptor interactions (Meng et al., 2014; Cordomi et al., 2015). In the membrane-spanning region, essentially every TM helix has been proposed as a potential interface (Selent and Kaczor, 2011; Ferre et al., 2014). For example, in the case of the A_{2A}R–D₂R heteromer, Canals et al. (2003) proposed that the TM interface was mainly composed of TM-V/VI/VII (D₂R) and TM-III/IV (A_{2A}R) whereas the study by Borroto-Escuela et al. (2010b) predicted that TM-IV/V (D₂R) interacted with either

TM-IV/V (A_{2A}R) or TM-I/VII (A_{2A}R). In the current work, the interface of the A_{2A}R–D₂R heteromer was further characterized by probing the ability of peptides based on the TM helices of the A_{2A}R to interfere with receptor–receptor interactions. The TM-IV and TM-V peptides had the strongest effect on A_{2A}R–D₂R interactions. Combined with the corresponding data for the D₂R (Borroto-Escuela et al., 2010b), the results pointed to a primary interface involving TM-IV/V for both the A_{2A}R and D₂R, but may also involve interactions with TM-VI. This model is in agreement with the work of Canals et al. (2003), in which a chimera of the D₁- and D₂R subtypes was characterized. To probe the role of the TM region of the D₂R in heteromerization, Canals et al. (2003) replaced TM-V/VI and IL3 with the corresponding sequence of the D₁ subtype, which does not dimerize with the A_{2A}R. The D₂/D₁ chimera did not interact with the A_{2A}R, supporting a TM interface involving either TM-V, TM-VI, IL3 or a combination of these regions. These results are consistent with our experimental data for peptides corresponding to TM-V of the D₂R, which resulted in a reduction of heteromerization in BRET assays (Borroto-Escuela et al., 2010b). As TM-IV, TM-V, and TM-VI cannot be part of a single interface, TM-IV/V interactions were prioritized over those involving TM-V/VI based on the fact that the TM-VI peptide resulted in the smallest effects experimentally. In addition, the fact that the degree of A_{2A}R–D₂R heteromerization is not affected by receptor activation (Canals et al., 2003) makes an TM-V/VI interface less likely because this complex would not allow the large conformational changes in TM-VI required for G protein binding (Rasmussen et al., 2011b). An alternative interpretation is that the dimer interface changes upon activation, as proposed for the D₂R (Guo et al., 2005) and metabotropic glutamate receptor 2 homodimers (Xue et al., 2015). Although this is a more complex model, it is possible that there is an equilibrium between the TM-IV/V and TM-V/VI interfaces, which may be influenced by activation of either protomer. The results for the

TM peptides and predicted interactions are also in agreement with the recent findings by Navarro et al. (2018), which also identified TM-IV/V as the primary interface of the A_{2A}R–D₂R heterodimer.

With a more detailed map of the helices involved in A_{2A}R–D₂R heteromerization, specific residue interactions and their role in allosteric modulation of ligand binding can be probed. Previous studies have investigated the role of intracellular regions in A_{2A}R–D₂R heteromerization by site directed mutagenesis. Based on pulldown and mass spectrometry experiments, negatively charged residues in the C-terminal tail of the A_{2A}R were proposed to form strong interactions with an arginine rich region in IL3 of the D₂R (Ciruela et al., 2004). Mutagenesis of the set of arginine residues in IL3 of the D₂R (217–222 and 267–269) to alanine abolished the negative allosteric modulation of D₂R agonist on activation of the A_{2A}R (Fernandez-Duenas et al., 2012). Similarly, site-directed mutagenesis for three residues in the C-terminal tail of the A_{2A}R (Ser374, Asp401, and Asp402) supported a role of this intracellular region in heteromerization. Loss of heteromerization for the alanine mutant of phosphorylated Ser374, the double mutant Asp401Ala/Asp402Ala as well as the combination of these three mutations were demonstrated in BRET assays. The two mutants involving Ser374 also disrupted the negative allosteric modulation mediated by the A_{2A}R on high-affinity agonist binding to the D₂R (Borroto-Escuela et al., 2010a). The C-terminal of the A_{2A}R and IL3 of the D₂R were not included in our proposed heterodimer model because of the lack of reliable templates to predict these regions. However, it should be noted that the positively charged region in IL3 of the D₂R is close to our proposed TM-IV/V interface as these residues are located at the intracellular part of TM-V. Considering that the three negatively charged residues of the A_{2A}R are located at the end of the long C-terminal tail, interactions between these two regions are also compatible with our proposed model.

To further test the predicted TM interface of the A_{2A}R–D₂R complex, two D₂R variants with mutations in either the N- or C-terminal end of TM-V were evaluated experimentally. None of these mutations disrupted dimerization completely, which was expected considering the large predicted contact surface and the involvement of intracellular regions in receptor–receptor interactions. The BRET data indicated a reduced population of heteroreceptor complexes, which supports the view that TM-V of the D₂R is part of the interface. The lack of effect in the PLA experiments may be due to a combination of the relatively modest impact of the mutants on dimerization and high receptor expression, which can lead to saturation effects that influence quantification of small differences in the level of receptor–receptor interactions using this technique (Mocanu et al., 2011). Based on the binding data, the predicted TM-IV/V interactions between the two receptors could contribute to the negative allosteric modulation across the A_{2A}R–D₂R heterodimer. Interestingly, crystal structures of the A_{2A}R in active- and inactive-like conformations suggest that TM-V shifts slightly inward upon activation by adenosine (Lebon et al., 2011). A similar inward contraction of TM-V was observed

for monoamine-recognizing GPCRs that are homologous to the D₂R (e.g., for the β_1 and β_2 adrenergic receptors) (Rasmussen et al., 2011a; Warne et al., 2011). The negative allosteric modulation across the A_{2A}R–D₂R heterodimer may thus be partly accomplished via interactions across the TM-V interface. The reduction of agonist binding to the D₂R observed upon activation of the A_{2A}R may be due to altered helix–helix interactions when TM-V shifts inward in response to adenosine receptor activation. In the complex with an A_{2A}R antagonist, TM-V can instead contribute to stabilizing the high affinity state conformation of the D₂R binding site, leading to the increased dopaminergic D₂R signaling sought in treatment of Parkinson's disease (Fuxe et al., 2007b; Armentero et al., 2011).

The A_{2A}R and D₂R exist both as homo- and heteromers in the brain and alteration of the balance between these receptor complexes influences intracellular signaling and could lead to development of neurological diseases (Fuxe and Borroto-Escuela, 2016). The heteromer interface between the A_{2A}R and D₂R was the main focus of this work. Future studies need to consider potential changes to the interface upon receptor activation, the influence of homodimers on A_{2A}R–D₂R interactions, and the existence of tetramers composed by A_{2A}R–A_{2A}R and D₂R–D₂R complexes (Bonaventura et al., 2015). As a first step toward characterizing the A_{2A}R homodimer, the effects of peptides derived from TM-IV and TM-V of the A_{2A}R on this complex were evaluated experimentally. In contrast to the strong inhibition of dimerization observed with these peptides for the A_{2A}R–D₂R heteromer, there were no effects on A_{2A}R homomerization. The TM-IV^{A2A} and TM-V^{A2A} peptides hence selectively modulate the A_{2A}R–D₂R heteromer, which supports the view that the A_{2A}R homo- and A_{2A}R–D₂R heteromerization involve different helices.

In this work, we developed an approach for mapping the interfaces of GPCR dimers based on biophysical experiments in combination with protein–protein docking and MD simulations. The modeling of the A_{2A}R–D₂R heterodimer was guided by information from low-resolution experiments that identified helices involved in receptor–receptor interactions and led to a potential TM-IV/V interface. The proposed A_{2A}R–D₂R structure provides a starting-point for designing new experiments that can contribute to further refinement of the model and understanding of allosteric modulation at the molecular level. The same approach can likely be extended to the large number of class A GPCRs that have been shown to engage in receptor–receptor interactions.

AUTHOR CONTRIBUTIONS

DR, JK, MJ, AR, and JC designed, performed, analyzed, and interpreted all the molecular modeling studies. DB-E, WR-F, TL, and KF designed, performed, analyzed, and interpreted all laboratory experiments. All authors contributed to the writing of the manuscript.

FUNDING

This work was supported by grants from the Swedish Research Council (2013-5708 and 2017-4676), Åke Wibergs Stiftelse, and the Science for Life Laboratory to JC. The Sven och Lilly Lawski Foundation supported DR with a Postdoctoral Fellowship. This work was also supported by grants from the Swedish Medical Research Council (04X-715 and VR-link) to KF, and by Hjärnfonden (FO2016-0302) to DB-E. Computational

resources were provided by the Swedish National Infrastructure for Computing (SNIC).

SUPPLEMENTARY MATERIAL

The Supplementary Material for this article can be found online at: <https://www.frontiersin.org/articles/10.3389/fphar.2018.00829/full#supplementary-material>

REFERENCES

- Angers, S., Salahpour, A., and Bouvier, M. (2001). Biochemical and biophysical demonstration of GPCR oligomerization in mammalian cells. *Life Sci.* 68, 2243–2250. doi: 10.1016/S0024-3205(01)01012-8
- Armentero, M. T., Pinna, A., Ferre, S., Lanciego, J. L., Muller, C. E., and Franco, R. (2011). Past, present and future of A(2A) adenosine receptor antagonists in the therapy of Parkinson's disease. *Pharmacol. Ther.* 132, 280–299. doi: 10.1016/j.pharmthera.2011.07.004
- Azad, K., Gall, D., Woods, A. S., Ledent, C., Ferre, S., and Schiffmann, S. N. (2009). Dopamine D₂ and adenosine A_{2A} receptors regulate NMDA-mediated excitation in accumbens neurons through A_{2A}-D₂ receptor heteromerization. *Neuropsychopharmacology* 34, 972–986. doi: 10.1038/npp.2008.144
- Berger, O., Edholm, O., and Jähnig, F. (1997). Molecular dynamics simulations of a fluid bilayer of dipalmitoylphosphatidylcholine at full hydration, constant pressure, and constant temperature. *Biophys. J.* 72, 2002–2013. doi: 10.1016/S0006-3495(97)78845-3
- Bonaventura, J., Navarro, G., Casado-Anguera, V., Azad, K., Rea, W., Moreno, E., et al. (2015). Allosteric interactions between agonists and antagonists within the adenosine A_{2A} receptor-dopamine D₂ receptor heterotetramer. *Proc. Natl. Acad. Sci. U.S.A.* 112, E3609–E3618. doi: 10.1073/pnas.1507704112
- Borroto-Escuela, D. O., Brito, I., Romero-Fernandez, W., Di Palma, M., Oflijan, J., Skieterska, K., et al. (2014). The G protein-coupled receptor heterodimer network (GPCR-HetNet) and its hub components. *Int. J. Mol. Sci.* 15, 8570–8590. doi: 10.3390/ijms15058570
- Borroto-Escuela, D. O., Flajolet, M., Agnati, L. F., Greengard, P., and Fuxe, K. (2013). Bioluminescence resonance energy transfer methods to study G protein-coupled receptor-receptor tyrosine kinase heteroreceptor complexes. *Methods Cell Biol.* 117, 141–164. doi: 10.1016/B978-0-12-408143-7.00008-6
- Borroto-Escuela, D. O., Hagman, B., Woolfenden, M., Pinton, L., Jiménez-Beristain, A., Oflijan, J., et al. (2016a). “In situ proximity ligation assay to study and understand the distribution and balance of GPCR homo- and heteroreceptor complexes in the brain,” in *Receptor and Ion Channel Detection in the Brain*, eds R. Lujan and F. Ciruela (Berlin: Springer), 109–126.
- Borroto-Escuela, D. O., Marcellino, D., Narvaez, M., Flajolet, M., Heintz, N., Agnati, L., et al. (2010a). A serine point mutation in the adenosine A_{2A}R C-terminal tail reduces receptor heteromerization and allosteric modulation of the dopamine D₂R. *Biochem. Biophys. Res. Commun.* 394, 222–227. doi: 10.1016/j.bbrc.2010.02.168
- Borroto-Escuela, D. O., Narvaez, M., Perez-Alea, M., Tarakanov, A. O., Jimenez-Beristain, A., Mudo, G., et al. (2015a). Evidence for the existence of FGFR1-5-HT_{1A} heteroreceptor complexes in the midbrain raphe 5-HT system. *Biochem. Biophys. Res. Commun.* 456, 489–493. doi: 10.1016/j.bbrc.2014.11.112
- Borroto-Escuela, D. O., Perez-Alea, M., Narvaez, M., Tarakanov, A. O., Mudo, G., Jimenez-Beristain, A., et al. (2015b). Enhancement of the FGFR1 signaling in the FGFR1-5-HT_{1A} heteroreceptor complex in midbrain raphe 5-HT neuron systems. Relevance for neuroplasticity and depression. *Biochem. Biophys. Res. Commun.* 463, 180–186. doi: 10.1016/j.bbrc.2015.04.133
- Borroto-Escuela, D. O., Pintsuk, J., Schafer, T., Friedland, K., Ferraro, L., Tanganelli, S., et al. (2016b). Multiple D₂ heteroreceptor complexes: new targets for treatment of schizophrenia. *Ther. Adv. Psychopharmacol.* 6, 77–94. doi: 10.1177/2045125316637570
- Borroto-Escuela, D. O., Romero-Fernandez, W., Tarakanov, A. O., Gomez-Soler, M., Corrales, F., Marcellino, D., et al. (2010b). Characterization of the A_{2A}R-D₂R interface: focus on the role of the C-terminal tail and the transmembrane helices. *Biochem. Biophys. Res. Commun.* 402, 801–807. doi: 10.1016/j.bbrc.2010.10.122
- Borroto-Escuela, D. O., Romero-Fernandez, W., Mudo, G., Perez-Alea, M., Ciruela, F., Tarakanov, A. O., et al. (2012). Fibroblast growth factor receptor 1-5-hydroxytryptamine 1A heteroreceptor complexes and their enhancement of hippocampal plasticity. *Biol. Psychiatry* 71, 84–91. doi: 10.1016/j.biopsych.2011.09.012
- Borroto-Escuela, D. O., Wydra, K., Li, X., Rodriguez, D., Carlsson, J., Jastrzebska, J., et al. (2018). Disruption of A_{2A}R-D₂R heteroreceptor complexes after A_{2A}R transmembrane 5 peptide administration enhances cocaine self-administration in rats. *Mol. Neurobiol.* doi: 10.1007/s12035-018-0887-1 [Epub ahead of print].
- Canals, M., Marcellino, D., Fanelli, F., Ciruela, F., De Benedetti, P., Goldberg, S. R., et al. (2003). Adenosine A_{2A}-dopamine D₂ receptor-receptor heteromerization: qualitative and quantitative assessment by fluorescence and bioluminescence energy transfer. *J. Biol. Chem.* 278, 46741–46749. doi: 10.1074/jbc.M306451200
- Chakrabarti, N., Neale, C., Payandeh, J., Pai, E. F., and Pomès, R. (2010). An iris-like mechanism of pore dilation in the CorA magnesium transport system. *Biophys. J.* 98, 784–792. doi: 10.1016/j.bpj.2009.11.009
- Chien, E. Y., Liu, W., Zhao, Q., Katritch, V., Han, G. W., Hanson, M. A., et al. (2010). Structure of the human dopamine D₃ receptor in complex with a D₂/D₃ selective antagonist. *Science* 330, 1091–1095. doi: 10.1126/science.1197410
- Ciruela, F., Burgueno, J., Casado, V., Canals, M., Marcellino, D., Goldberg, S. R., et al. (2004). Combining mass spectrometry and pull-down techniques for the study of receptor heteromerization. Direct epitope-epitope electrostatic interactions between adenosine A_{2A} and dopamine D₂ receptors. *Anal. Chem.* 76, 5354–5363. doi: 10.1021/ac049295f
- Cordomi, A., Navarro, G., Aymerich, M. S., and Franco, R. (2015). Structures for G-protein-coupled receptor tetramers in complex with G proteins. *Trends Biochem. Sci.* 40, 548–551. doi: 10.1016/j.tibs.2015.07.007
- Darden, T., York, D., and Pedersen, L. (1993). Particle mesh Ewald: an N-log(N) method for Ewald sums in large systems. *J. Chem. Phys.* 98, 10089–10089. doi: 10.1063/1.464397
- Dasgupta, S., Ferre, S., Kull, B., Hedlund, P. B., Finnman, U. B., Ahlberg, S., et al. (1996). Adenosine A_{2A} receptors modulate the binding characteristics of dopamine D₂ receptors in stably cotransfected fibroblast cells. *Eur. J. Pharmacol.* 316, 325–331. doi: 10.1016/S0014-2999(96)00665-6
- Davis, I. W., Leaver-Fay, A., Chen, V. B., Block, J. N., Kapral, G. J., Wang, X., et al. (2007). MolProbity: all-atom contacts and structure validation for proteins and nucleic acids. *Nucleic Acids Res.* 35, W375–W383. doi: 10.1093/nar/gkm216
- Dominguez, C., Boelens, R., and Bonvin, A. M. (2003). HADDOCK: a protein-protein docking approach based on biochemical or biophysical information. *J. Am. Chem. Soc.* 125, 1731–1737. doi: 10.1021/ja026939x
- Feltmann, K., Borroto-Escuela, D. O., Ruegg, J., Pinton, L., De Oliveira Sergio, T., Narvaez, M., et al. (2018). Effects of long-term alcohol drinking on the dopamine D₂ receptor: gene expression and heteroreceptor complexes in the striatum in rats. *Alcohol. Clin. Exp. Res.* 42, 338–351. doi: 10.1111/acer.13568
- Fenu, S., Pinna, A., Ongini, E., and Morelli, M. (1997). Adenosine A_{2A} receptor antagonism potentiates L-DOPA-induced turning behaviour and c-fos expression in 6-hydroxydopamine-lesioned rats. *Eur. J. Pharmacol.* 321, 143–147. doi: 10.1016/S0014-2999(96)00944-2
- Fernandez-Duenas, V., Gomez-Soler, M., Jacobson, K. A., Kumar, S. T., Fuxe, K., Borroto-Escuela, D. O., et al. (2012). Molecular determinants of A_{2A}R-D₂R allosterism: role of the intracellular loop 3 of the D₂R. *J. Neurochem.* 123, 373–384. doi: 10.1111/j.1471-4159.2012.07956.x

- Ferre, S., Casado, V., Devi, L. A., Filizola, M., Jockers, R., Lohse, M. J., et al. (2014). G protein-coupled receptor oligomerization revisited: functional and pharmacological perspectives. *Pharmacol. Rev.* 66, 413–434. doi: 10.1124/pr.113.008052
- Ferre, S., Von Euler, G., Johansson, B., Fredholm, B. B., and Fuxe, K. (1991). Stimulation of high-affinity adenosine A₂ receptors decreases the affinity of dopamine D₂ receptors in rat striatal membranes. *Proc. Natl. Acad. Sci. U.S.A.* 88, 7238–7241. doi: 10.1073/pnas.88.16.7238
- Franco, R., Ferre, S., Agnati, L., Torvinen, M., Gines, S., Hillion, J., et al. (2000). Evidence for adenosine/dopamine receptor interactions: indications for heteromerization. *Neuropsychopharmacology* 23, S50–S59. doi: 10.1016/S0893-133X(00)00144-5
- Fuxe, K., and Borroto-Escuela, D. O. (2016). Heteroreceptor complexes and their allosteric receptor-receptor interactions as a novel biological principle for integration of communication in the CNS: targets for drug development. *Neuropsychopharmacology* 41, 380–382. doi: 10.1038/npp.2015.244
- Fuxe, K., Borroto-Escuela, D. O., Romero-Fernandez, W., Palkovits, M., Tarakanov, A. O., Ciruela, F., et al. (2014). Moonlighting proteins and protein-protein interactions as neurotherapeutic targets in the G protein-coupled receptor field. *Neuropsychopharmacology* 39, 131–155. doi: 10.1038/npp.2013.242
- Fuxe, K., Ferre, S., Canals, M., Torvinen, M., Terasmaa, A., Marcellino, D., et al. (2005). Adenosine A_{2A} and dopamine D₂ heteromeric receptor complexes and their function. *J. Mol. Neurosci.* 26, 209–220. doi: 10.1385/JMN
- Fuxe, K., Ferre, S., Genedani, S., Franco, R., and Agnati, L. F. (2007a). Adenosine receptor-dopamine receptor interactions in the basal ganglia and their relevance for brain function. *Physiol. Behav.* 92, 210–217. doi: 10.1016/j.physbeh.2007.05.034
- Fuxe, K., Guidolin, D., Agnati, L. F., and Borroto-Escuela, D. O. (2015). Dopamine heteroreceptor complexes as therapeutic targets in Parkinson's disease. *Expert Opin. Ther. Targets* 19, 377–398. doi: 10.1517/14728222.2014.981529
- Fuxe, K., Marcellino, D., Borroto-Escuela, D. O., Guescini, M., Fernandez-Duenas, V., Tanganelli, S., et al. (2010). Adenosine-dopamine interactions in the pathophysiology and treatment of CNS disorders. *CNS Neurosci. Ther.* 16, e18–e42. doi: 10.1111/j.1755-5949.2009.00126.x
- Fuxe, K., Marcellino, D., Genedani, S., and Agnati, L. (2007b). Adenosine A(2A) receptors, dopamine D(2) receptors and their interactions in Parkinson's disease. *Mov. Disord.* 22, 1990–2017. doi: 10.1002/mds.21440
- Granier, S., Manglik, A., Kruse, A. C., Kobilka, T. S., Thian, F. S., Weis, W. I., et al. (2012). Structure of the delta-opioid receptor bound to naltrindole. *Nature* 485, 400–404. doi: 10.1038/nature11111
- Guitart, X., Navarro, G., Moreno, E., Yano, H., Cai, N. S., Sanchez-Soto, M., et al. (2014). Functional selectivity of allosteric interactions within G protein-coupled receptor oligomers: the dopamine D₁-D₃ receptor heterotetramer. *Mol. Pharmacol.* 86, 417–429. doi: 10.1124/mol.114.093096
- Guo, W., Shi, L., Filizola, M., Weinstein, H., and Javitch, J. A. (2005). Crosstalk in G protein-coupled receptors: changes at the transmembrane homodimer interface determine activation. *Proc. Natl. Acad. Sci. U.S.A.* 102, 17495–17500. doi: 10.1073/pnas.0508950102
- Han, Y., Moreira, I. S., Urizar, E., Weinstein, H., and Javitch, J. A. (2009). Allosteric communication between protomers of dopamine class A GPCR dimers modulates activation. *Nat. Chem. Biol.* 5, 688–695. doi: 10.1038/nchembio.199
- Hasbi, A., Fan, T., Alijaniam, M., Nguyen, T., Perreault, M. L., O'dowd, B. F., et al. (2009). Calcium signaling cascade links dopamine D₁-D₂ receptor heteromer to striatal BDNF production and neuronal growth. *Proc. Natl. Acad. Sci. U.S.A.* 106, 21377–21382. doi: 10.1073/pnas.0903676106
- Hasbi, A., Perreault, M. L., Shen, M. Y. F., Fan, T., Nguyen, T., Alijaniam, M., et al. (2017). Activation of dopamine D₁-D₂ receptor complex attenuates cocaine reward and reinstatement of cocaine-seeking through inhibition of DARPP-32, ERK, and DeltaFosB. *Front. Pharmacol.* 8:924. doi: 10.3389/fphar.2017.00924
- Hebert, T. E., Moffett, S., Morello, J. P., Loisel, T. P., Bichet, D. G., Barret, C., et al. (1996). A peptide derived from a beta₂-adrenergic receptor transmembrane domain inhibits both receptor dimerization and activation. *J. Biol. Chem.* 271, 16384–16392. doi: 10.1074/jbc.271.27.16384
- Hess, B., Bekker, H., Berendsen, H. J. C., and Fraaije, J. G. E. M. (1997). LINC: a linear constraint solver for molecular simulations. *J. Comput. Chem.* 18, 1463–1472. doi: 10.1002/(SICI)1096-987X(199709)18:12<1463::AID-JCC4>3.0.CO;2-H
- Hillion, J., Canals, M., Torvinen, M., Casado, V., Scott, R., Terasmaa, A., et al. (2002). Coaggregation, cointernalization, and codesensitization of adenosine A_{2A} receptors and dopamine D₂ receptors. *J. Biol. Chem.* 277, 18091–18097. doi: 10.1074/jbc.M107731200
- Huang, J., Chen, S., Zhang, J. J., and Huang, X. Y. (2013). Crystal structure of oligomeric beta₁-adrenergic G protein-coupled receptors in ligand-free basal state. *Nat. Struct. Mol. Biol.* 20, 419–425. doi: 10.1038/nsmb.2504
- Isberg, V., De Graaf, C., Bortolato, A., Cherezov, V., Katritch, V., Marshall, F. H., et al. (2015). Generic GPCR residue numbers - aligning topology maps while minding the gaps. *Trends Pharmacol. Sci.* 36, 22–31. doi: 10.1016/j.tips.2014.11.001
- Jastrzebska, B., Chen, Y., Orban, T., Jin, H., Hofmann, L., and Palczewski, K. (2015). Disruption of rhodopsin dimerization with synthetic peptides targeting an interaction interface. *J. Biol. Chem.* 290, 25728–25744. doi: 10.1074/jbc.M115.662684
- Jorgensen, W., Chandrasekhar, J., Madura, J., Rw, I., and Klein, M. (1983). Comparison of simple potential functions for simulating liquid water. *J. Chem. Phys.* 79, 926–935. doi: 10.1063/1.445869
- Jorgensen, W. L., Maxwell, D. S., and Tirado-Rives, J. (1996). Development and testing of the OPLS all-atom force field on conformational energetics and properties of organic liquids. *J. Am. Chem. Soc.* 118, 11225–11236. doi: 10.1021/ja9621760
- Kamiya, T., Saitoh, O., Yoshioka, K., and Nakata, H. (2003). Oligomerization of adenosine A_{2A} and dopamine D₂ receptors in living cells. *Biochem. Biophys. Res. Commun.* 306, 544–549. doi: 10.1016/S0006-291X(03)00991-4
- Lagerstrom, M. C., and Schioth, H. B. (2008). Structural diversity of G protein-coupled receptors and significance for drug discovery. *Nat. Rev. Drug Discov.* 7, 339–357. doi: 10.1038/nrd2518
- Lazarova, T., Brewin, K. A., Stoeber, K., and Robinson, C. R. (2004). Characterization of peptides corresponding to the seven transmembrane domains of human adenosine A_{2A} receptor. *Biochemistry* 43, 12945–12954. doi: 10.1021/bi0492051
- Lebon, G., Warne, T., Edwards, P. C., Bennett, K., Langmead, C. J., Leslie, A. G., et al. (2011). Agonist-bound adenosine A_{2A} receptor structures reveal common features of GPCR activation. *Nature* 474, 521–525. doi: 10.1038/nature10136
- Lee, L. T. O., Ng, S. Y. L., Chu, J. Y. S., Sekar, R., Harikumar, K. G., Miller, L. J., et al. (2014). Transmembrane peptides as unique tools to demonstrate the in vivo action of a cross-class GPCR heterocomplex. *FASEB J.* 28, 2632–2644. doi: 10.1096/fj.13-246868
- Lefkowitz, R. J. (2004). Historical review: a brief history and personal retrospective of seven-transmembrane receptors. *Trends Pharmacol. Sci.* 25, 413–422. doi: 10.1016/j.tips.2004.06.006
- Liu, W., Chun, E., Thompson, A. A., Chubukov, P., Xu, F., Katritch, V., et al. (2012). Structural basis for allosteric regulation of GPCRs by sodium ions. *Science* 337, 232–236. doi: 10.1126/science.1219218
- Manglik, A., Kruse, A. C., Kobilka, T. S., Thian, F. S., Mathiesen, J. M., Sunahara, R. K., et al. (2012). Crystal structure of the micro-opioid receptor bound to a morphinan antagonist. *Nature* 485, 321–326. doi: 10.1038/nature10954
- Marsango, S., Varela, M. J., and Milligan, G. (2015). Approaches to characterize and quantify oligomerization of GPCRs. *Methods Mol. Biol.* 1335, 95–105. doi: 10.1007/978-1-4939-2914-6-7
- Martinez-Munoz, L., Rodriguez-Frade, J. M., and Mellado, M. (2016). Use of resonance energy transfer techniques for in vivo detection of chemokine receptor oligomerization. *Methods Mol. Biol.* 1407, 341–359. doi: 10.1007/978-1-4939-3480-5-24
- Meng, X. Y., Mezei, M., and Cui, M. (2014). Computational approaches for modeling GPCR dimerization. *Curr. Pharm. Biotechnol.* 15, 996–1006. doi: 10.2174/1389201015666141013102515
- Miyamoto, S., and Kollman, P. A. (1992). Settle: an analytical version of the SHAKE and RATTLE algorithm for rigid water models. *J. Comput. Chem.* 13, 952–962. doi: 10.1002/jcc.540130805
- Mocanu, M. M., Varadi, T., Szollosi, J., and Nagy, P. (2011). Comparative analysis of fluorescence resonance energy transfer (FRET) and proximity ligation assay (PLA). *Proteomics* 11, 2063–2070. doi: 10.1002/pmic.201100028
- Murakami, M., and Kouyama, T. (2008). Crystal structure of squid rhodopsin. *Nature* 453, 363–367. doi: 10.1038/nature06925
- Navarro, G., Cordomi, A., Casado-Anguera, V., Moreno, E., Cai, N. S., Cortes, A., et al. (2018). Evidence for functional pre-coupled complexes of receptor

- heteromers and adenylyl cyclase. *Nat. Commun.* 9:1242. doi: 10.1038/s41467-018-03522-3
- Navarro, G., Ferre, S., Cordomi, A., Moreno, E., Mallol, J., Casado, V., et al. (2010). Interactions between intracellular domains as key determinants of the quaternary structure and function of receptor heteromers. *J. Biol. Chem.* 285, 27346–27359. doi: 10.1074/jbc.M110.115634
- Ng, G. Y., O'dowd, B. F., Lee, S. P., Chung, H. T., Brann, M. R., Seeman, P., et al. (1996). Dopamine D₂ receptor dimers and receptor-blocking peptides. *Biochem. Biophys. Res. Commun.* 227, 200–204. doi: 10.1006/bbrc.1996.1489
- Overton, M. C., and Blumer, K. J. (2000). G-protein-coupled receptors function as oligomers in vivo. *Curr. Biol.* 10, 341–344. doi: 10.1016/S0960-9822(00)00386-9
- Parrinello, M., and Rahman, A. (1981). Polymorphic transitions in single-crystals - a new molecular-dynamics method. *J. Appl. Phys.* 52, 7182–7190. doi: 10.1063/1.328693
- Pfleger, K. D., and Eidne, K. A. (2006). Illuminating insights into protein-protein interactions using bioluminescence resonance energy transfer (BRET). *Nat. Methods* 3, 165–174. doi: 10.1038/nmeth841
- Pronk, S., Páll, S., Schulz, R., Larsson, P., Bjelkmar, P., Apostolov, R., et al. (2013). GROMACS 4.5: a high-throughput and highly parallel open source molecular simulation toolkit. *Bioinformatics* 29, 845–854. doi: 10.1093/bioinformatics/btt055
- Rasmussen, S. G., Choi, H. J., Fung, J. J., Pardon, E., Casarosa, P., Chae, P. S., et al. (2011a). Structure of a nanobody-stabilized active state of the beta(2) adrenoceptor. *Nature* 469, 175–180. doi: 10.1038/nature09648
- Rasmussen, S. G., Devree, B. T., Zou, Y., Kruse, A. C., Chung, K. Y., Kobilka, T. S., et al. (2011b). Crystal structure of the beta2 adrenergic receptor-Gs protein complex. *Nature* 477, 549–555. doi: 10.1038/nature10361
- Rico, A. J., Dopeso-Reyes, I. G., Martínez-Pinilla, E., Sucunza, D., Pignataro, D., Roda, E., et al. (2017). Neurochemical evidence supporting dopamine D₁-D₂ receptor heteromers in the striatum of the long-tailed macaque: changes following dopaminergic manipulation. *Brain Struct. Funct.* 222, 1767–1784. doi: 10.1007/s00429-016-1306-x
- Rodrigues, J. P., Trellet, M., Schmitz, C., Kastrits, P., Karaca, E., Melquiond, A. S., et al. (2012). Clustering biomolecular complexes by residue contacts similarity. *Proteins* 80, 1810–1817. doi: 10.1002/prot.24078
- Rodríguez, D., Bello, X., and Gutiérrez-De-Terán, H. (2012). Molecular modelling of G protein-coupled receptors through the web. *Mol. Inform.* 31, 334–341. doi: 10.1002/minf.201100162
- Rodríguez, D., and Gutierrez-De-Teran, H. (2012). Characterization of the homodimerization interface and functional hotspots of the CXCR4 chemokine receptor. *Proteins* 80, 1919–1928. doi: 10.1002/prot.24099
- Sali, A., and Blundell, T. L. (1993). Comparative protein modelling by satisfaction of spatial restraints. *J. Mol. Biol.* 234, 779–815. doi: 10.1006/jmbi.1993.1626
- Schwarzschild, M. A., Agnati, L., Fuxe, K., Chen, J. F., and Morelli, M. (2006). Targeting adenosine A_{2A} receptors in Parkinson's disease. *Trends Neurosci.* 29, 647–654. doi: 10.1016/j.tins.2006.09.004
- Selent, J., and Kaczor, A. A. (2011). Oligomerization of G protein-coupled receptors: computational methods. *Curr. Med. Chem.* 18, 4588–4605. doi: 10.2174/092986711797379320
- Shen, M. Y., and Sali, A. (2006). Statistical potential for assessment and prediction of protein structures. *Protein Sci.* 15, 2507–2524. doi: 10.1110/ps.062416606
- Thevenin, D., and Lazarova, T. (2008). Stable interactions between the transmembrane domains of the adenosine A_{2A} receptor. *Protein Sci.* 17, 1188–1199. doi: 10.1110/ps.034843.108
- Thevenin, D., Roberts, M. F., Lazarova, T., and Robinson, C. R. (2005). Identifying interactions between transmembrane helices from the adenosine A_{2A} receptor. *Biochemistry* 44, 16239–16245. doi: 10.1021/bi051422u
- Vidi, P. A., Przybyla, J. A., Hu, C. D., and Watts, V. J. (2010). Visualization of G protein-coupled receptor (GPCR) interactions in living cells using bimolecular fluorescence complementation (BiFC). *Curr. Protoc. Neurosci.* 51, 5.29.1–5.29.15. doi: 10.1002/0471142301.ns0529s51
- Vinals, X., Moreno, E., Lanfumey, L., Cordomi, A., Pastor, A., De La Torre, R., et al. (2015). Cognitive impairment induced by Delta9-tetrahydrocannabinol occurs through heteromers between cannabinoid CB1 and serotonin 5-HT_{2A} receptors. *PLoS Biol.* 13:e1002194. doi: 10.1371/journal.pbio.1002194
- Wang, S., Che, T., Levit, A., Shoichet, B. K., Wacker, D., and Roth, B. L. (2018). Structure of the D₂ dopamine receptor bound to the atypical antipsychotic drug risperidone. *Nature* 555, 269–273. doi: 10.1038/nature25758
- Warne, T., Moukhametzianov, R., Baker, J. G., Nehme, R., Edwards, P. C., Leslie, A. G., et al. (2011). The structural basis for agonist and partial agonist action on a beta(1)-adrenergic receptor. *Nature* 469, 241–244. doi: 10.1038/nature09746
- Wu, B., Chien, E. Y., Mol, C. D., Fenalti, G., Liu, W., Katritch, V., et al. (2010). Structures of the CXCR4 chemokine GPCR with small-molecule and cyclic peptide antagonists. *Science* 330, 1066–1071. doi: 10.1126/science.1194396
- Xue, L., Rovira, X., Scholler, P., Zhao, H., Liu, J., Pin, J. P., et al. (2015). Major ligand-induced rearrangement of the heptahelical domain interface in a GPCR dimer. *Nat. Chem. Biol.* 11, 134–140. doi: 10.1038/nchembio.1711
- Yang, S. N., Dasgupta, S., Lledo, P. M., Vincent, J. D., and Fuxe, K. (1995). Reduction of dopamine D₂ receptor transduction by activation of adenosine A_{2a} receptors in stably A_{2a}/D₂ (long-form) receptor co-transfected mouse fibroblast cell lines: studies on intracellular calcium levels. *Neuroscience* 68, 729–736. doi: 10.1016/0306-4522(95)00171-E

Conflict of Interest Statement: The authors declare that the research was conducted in the absence of any commercial or financial relationships that could be construed as a potential conflict of interest.

Copyright © 2018 Borroto-Escuela, Rodríguez, Romero-Fernandez, Kapla, Jaiteh, Ranganathan, Lazarova, Fuxe and Carlsson. This is an open-access article distributed under the terms of the Creative Commons Attribution License (CC BY). The use, distribution or reproduction in other forums is permitted, provided the original author(s) and the copyright owner(s) are credited and that the original publication in this journal is cited, in accordance with accepted academic practice. No use, distribution or reproduction is permitted which does not comply with these terms.